Electrodeposition of One-Dimensional Nanostructures: Environmentally Friendly Method

Vicente de Oliveira Sousa Neto[1,*], Gilberto Dantas Saraiva[2], A. J. Ramiro de Castro[3], Paulo de Tarso Cavalcante Freire[3], and Ronaldo Ferreira do Nascimento[4,*]

[1]*Laboratory of Study and Research in Pollutants Removal by Adsorption – LERPAD, Department of Chemistry – State University of Ceara (UECE-FECLESC), Rua José´ de Queiroz Pessoa, N1 2554 – University Plateau –CEP: 63.900-000 – Quixada´/CE, Brazil;* [2]*Laboratory of Synthesis and Characterization of Materials – LASCAM, Department of Physics, State. University of Ceara´ (UECE-FECLESC), Rua José´ de Queiroz Pessoa, N1 2554 – University Plateau – CEP: 63.900-000 – Quixada´/CE, Brazil;* [3]*Crystal Characterization and Processing Laboratory, Department of Physics, Federal University of Ceara – UFC, Fortaleza, Brazil and Physics - Federal University of Ceará -Brazil ;Federal University of Ceara´ – UFC, Quixada/CE Av. José´ de Freitas Queiroz, 5003, Quixada´ – CE, 63902-580, Brazil;* [4]*Laboratory of Trace Analysis (LAT) – Department of Analytical and Physical Chemistry, Federal University of Ceara – UFC, Fortaleza, Brazil*

Abstract: During the past decade, nanotechnology has become an active field of research because of its huge potential for a variety of applications. When the size of many established, well-studied materials is reduced to the nanoscale, radically improved or new surprising properties often emerge. There are mainly four types of nanostructures: zero, one, two and three dimensional structures. Among them, one-dimensional (1D) nanostructures have been the focus of quite extensive studies worldwide, partially because of their unique physical and chemical properties. Compared to the other three dimensional structures, the first characteristic of 1D nanostructure is its smaller dimension structure and high aspect ratio, which could efficiently transport electrical carriers along one controllable direction; as a consequence they are highly suitable for moving charges in integrated nanoscale systems. The second characteristic of 1D nanostructure is its device function, which can be exploited as device elements in many kinds of nanodevices. Indeed it is important to note that superior physical properties including superconductivity, enhanced magnetic coercivity and the unusual magnetic state of some 1D nanostructures have been theoretically predicted and some of them have already been confirmed by experiments. In order to attain the potential offered by 1D nanostructures, one of the most important issues is how to synthesize 1D nanostructures in large quantities with a convenient method. Many synthetic strategies, such as solution or vapor-phase approaches, template-directed methods, electrospinning techniques, solvothermal syntheses, self-assembly methods, etc., have been developed to fabricate different classes of 1D nanostructured materials, including metals, semiconductors, functional oxides, structural ceramics, polymers and composites. All the methods can be divided into two categories: those carried out in a gas phase (*i.e.*, "dry processes") and those carried out in a liquid phase (*i.e.*, "wet processes"). The dry processes include, for example, techniques such as chemical vapor deposition (CVD), physical vapor deposition (PVD), pulse laser deposition (PLD), metal-organic chemical vapor deposition (MOCVD), and molecular beam epitaxy (MBE). In general, these gas phase processes require expensive and specialized equipments. The wet processes include sol-gel method, hydrothermal method, chemical bath deposition (CBD) and electrodeposition. Among the above mentioned methods, electrodeposition has many advantages such as low cost, environmentally friendly, high growth rate at relatively low temperatures and easier control of shape and size. Generally, there are two strategies to produce the 1D nanostructures through the electrochemical process. They are the template-assisted electrodeposition, and the template-free electrodeposition. In this chapter, we will approach the recent progress and offer some prospects of future directions in electrodeposition of 1D nanostructures. Electrodeposition is a simple and flexible method for the synthesis of one-dimensional (1D) nanostructures and has attracted great attention in recent years.

Keywords: Nanostructures, Environmentally friendly, Electrodeposition.

INTRODUCTION

Nanotechnology has already presented a profound impact on global economy and society in the twenty-first century. It plays an important role in the development and advancement of strategic areas such as materials engineering and manufacturing, physics and chemistry, electronics, medicine, energy and environment, biotechnology and information technology (Figure **1**). [1-3]. Several countries have devoted substantial resources to the development of nanotechnology as a government strategy. In 2018, the South Korea invested US $ 626.0 million in nanotech. The European Union allocated an investment of US $ 140.02 million in 2019 in the same segment. The United States, despite a 5.5% reduction in investment in nanotechnology compared to 2018, still leads nanotechnology investments with a government budget proposal of $ 1,395.6 million in 2019 (NNI, 2019).

In the past few years, one-dimensional (1D) nanostructures, including nanowires, nanorods, nanotubes and nanoribbons, have been intensively studied owing to their novel physical properties and
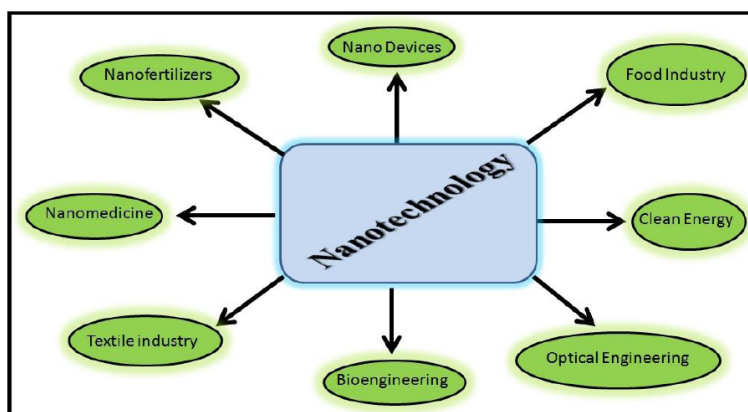
Figure 1: Aplication of nanotechnology. This file by Vicente Neto is licensed under the Creative Commons Attribution-Share Alike 4.0. Link https://commons.wikimedia.org/wiki/File:Application_of_nanotechnology.jpg.

fascinating potential applications in the future nanodevices. In fact, through nanoscience, it was noted that the size of a material is of fundamental importance in determining its properties, probably due to the different ways in which electrons interact in two-dimensional (2D) and one-dimensional (1D) structures [1-4]. The anisotropy inherent in quasi-1D and -2D systems is central to the unique properties and phases that these materials exhibit, although the small but finite interactions between 1D chains or 2D layers in bulk materials have made it difficult to address the interesting properties expected for the pure low-dimensional systems. Superior physical and chemical properties including superconductivity, enhanced magnetic coercivity and the unusual magnetic state of some 1D nanostructures have been theoretically predicted and some of them have already been confirmed by experiments [5]. When the size of many established, well-studied materials is reduced to the nanoscale, radically improved or new surprising properties often emerge. There are mainly four types of nanostructures: zero, one, two and three dimension structures. Among them, one-dimensional (1D) nanostructures have been the focus of quite extensive studies worldwide, partially because of their unique physical and chemical properties. Compared to the other three dimensional structures, one characteristic of 1D nanostructure is its smaller dimension structure and high aspect ratio, allowing efficiently transport electrical carriers along one controllable direction. As a consequence, we can imagine they are highly suitable for moving charges in integrated nanoscale systems [6].

Generally, there are two strategies to produce the 1D nanostructures through the electrochemical process. One is the template-assisted electrodeposition, where the 1D anisotropic growth is performed by using various templates to confine the growth space of the electrodeposits. The template-assisted electrodeposition has been demonstrated to be a versatile approach for the preparation of the 1D nanostructures of numerous materials, including metals [7], semiconductors [8] and conductive polymers [9]. Another strategy is the template-free electrodeposition, where the 1D anisotropic growth is achieved by utilizing the intrinsic anisotropic crystallographic structure of a targeted material.

To date, several 1D nanostructures have been obtained by the template-free electrodeposition. The following content is a review of the recent progress made with both the template-assisted and template-free electrochemical synthesis of the 1D nanostructures and offer some prospects of the future directions.

2. STRATEGIES FOR ACHIEVING 1D GROWTH

2.1. Template-Assisted Electrodeposition

Recently, the template-assisted fabrication of functional nanowires has attracted considerable attention. This is mainly owing to the possibility of controlling the length, diameter, and density of the fabricated nanowires by varying the template and/or deposition parameters. In the electrochemical process, a template is used to direct the 1D growth. The electrodeposition occurs at the surface of the electrode and the targeted material grows in the free space of the template to form 1D morphologies. The template method has been accomplished using a variety of templates, such as polycarbonate templates (PC), nanochannel alumina (NCA) and anodized aluminum oxides (AAO). It has been considered that the AAO template is an ideal template as it possesses many desirable characteristics, including tunable pore dimensions, good mechanical strength, thermal stability

and ordered nanotubes at a high density (10^9–10^{11}/cm^2) [10-14]. The template-assisted electrodeposition has been successfully used to prepare 1D nanostructures of various metals, semiconductors and conductive polymers.

2.1.2. Templates

The templates utilized for electrodeposition include (i) the so-called "hard" templates such as porous membranes with 1D channel and step edges present on the surfaces of a solid substrate and (ii) the "soft" templates such as mesoscale structures which are self-assembled from block copolymers, liquid crystal materials and surfactants. The formation of nanostructures in template-based synthesis results from growth of nuclei that invariably nucleate at the holes and defects of the electrode substrate. Subsequent growth of these nuclei at the template yields the desired surface morphology of the nanostructures, which can therefore be synthesized by choosing the appropriate surface of the electrode. Highly oriented pyrolitic graphite (HOPG) has been used extensively as an electrode substrate for the electrodeposition of silver [15-17], gold [18], molybdenum [19], palladium [20-22], and platinum [23] nanostructures.

2.1.2.1. Anodic Aluminum Oxide (AAO) Template

The protection or decoration of Al surfaces by anodization has been used commercially since at least 1923 [24]. Self-organized "nanopore" structures in anodic alumina films, called "alumite", have attracted great attention [25-27] due to their high pore density and their potential use for masking or information storage [28]. When the pores are filled with metals or semiconductors in a subsequent alternating-current reductive electrolysis, these films can be fabricated into interesting magnetic recording, electronic, and electrooptical devices [11-22, 29-31]. These "nanopores" can be used as templates for forming arrays of nanowires either embedded in alumite [32-34] or "freed" by a subsequent chemical removal of the alumite structure as shown in Figure **2** [35, 36].

In general, the AAO films can be formed with two different morphologies (*i.e.*, nonporous barrier-type oxide films and porous-type oxide films) depending mainly on the nature of the anodizing electrolyte [3]. Because the process was first implemented for protection purposes, the anodization of aluminum and its alloys, particularly porous-type anodization, has received considerable attention in the industry due its extensive practical applications. Many desirable engineering properties such as excellent hardness, corrosion and abrasion resistance can be obtained by anodizing aluminum metals in acid electrolytes [4]. In addition, due to their high porosity, the porous oxide films formed on the metals serve as a good adhesion base for electroplating, painting, and semi-permanent decorative coloration. The anodized products can be easily found in electronic gadgets, electrolytic capacitors, cookware, outdoor products, plasma equipments, vehicles, architectural materials, machine parts, etc.

Porous AAO film grown on aluminum is composed of a thin barrier oxide layer in conformal contact with aluminum, and an overlying, relatively thick, porous oxide film containing mutually parallel nanopores extends from the barrier oxide layer to the film surface [7]. Each cylindrical nanopore and its surrounding oxide region constitute a hexagonal cell aligned normal to the metal surface. Under specific electrochemical conditions, the oxide cells self-organize into hexagonal close-packed arrangement, forming a honeycomb-like structure [5-7]. Pore diameter and density of self-ordered porous AAOs are tunable in wide ranges by
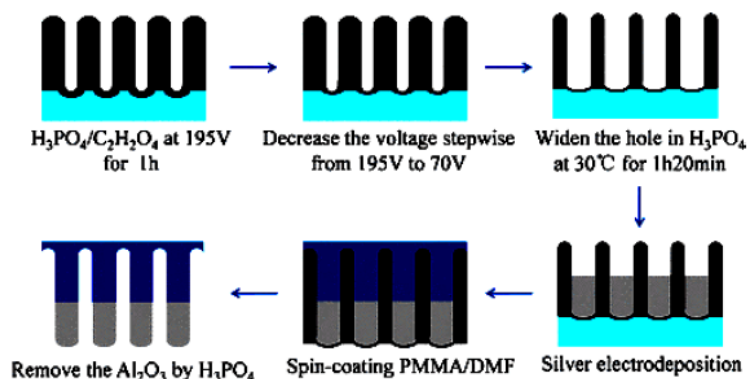
Figure 2: Fabrication procedure of silver nanorod arrays/PMMA composite (green: Al, black: PAA, gray: silver, blue: PMMA). PMMA: polymethyl methacrylate. From Li *et al*, 2017. This article is distributed under the terms of the Creative Commons Attribution 4.0 License. Link https://journals.sagepub.com/doi/full/10.1177/1847980417717543.

properly choosing anodization conditions: pore diameter = 10–400 nm and pore density = 10^8–10^{10} pores cm^{-2}. The novel and tunable structural features of porous AAOs have been intensively exploited for synthesizing a diverse range of nanostructured materials in the forms of nanodots, nanowires, and nanotubes, and also for developing functional nanodevices. In Figure **3** is shown a nanoporous-type oxide by electrodeposition.

2.1.2.2. Types of Anodic Aluminum Oxide (AAO)

Anodization of aluminum in aqueous electrolytes forms anodic oxide films with two different morphologies, that is, the nonporous barrier-type oxide films and the porous-type oxide films. The chemical nature of the electrolytes mainly determines the morphology of AAOs [37, 38]. A compact nonporous barrier-type AAO film can be formed in neutral electrolytes (pH 5-7), such as borate, oxalate, citrate, phosphate, adipate, tungstate solution, etc., in which the anodic oxide is practically insoluble [39]. Meanwhile, porous-type AAOs are formed in acidic electrolytes, such as selenic [40], sulphuric oxalic, phosphoric, chromic, as well as malonic, tartaric, citric and malic acids [41-44], etc., in which anodic oxide is slightly soluble. Early models describing anodic oxide growth were developed on the basis of the barrier-type oxide [45, 46, 47]. Moreover, in the early stage of porous-type oxide growth, the formation of the initial barrier oxide is followed by the emergence of incipient pores. Figure **4** shows two different types of anodic aluminum oxide (AAO) formed.
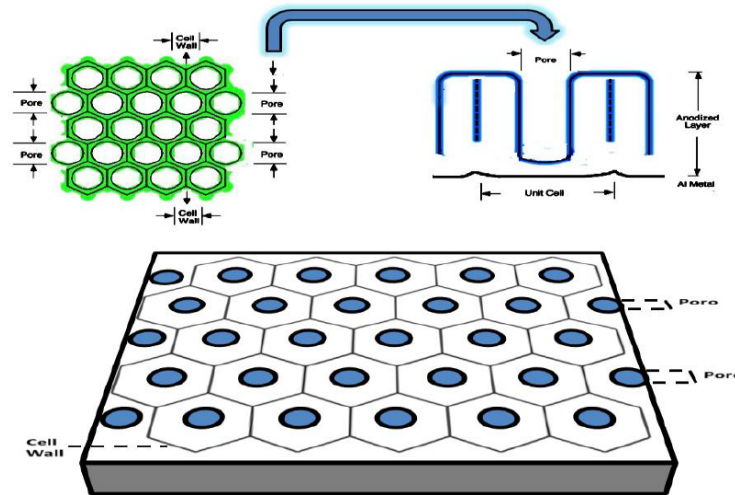
Figure 3: Porous-type AAO. This figure by Vicente Neto is licensed under the Creative Commons Attribution 4.0 International https://commons.wikimedia.org/wiki/File:Porous-type_oxide_films.jpg.
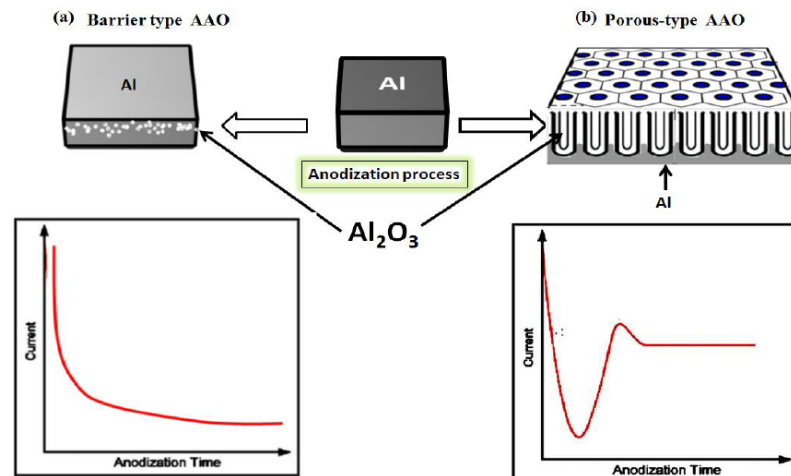
Figure 4: Two different types of anodic aluminum oxide (AAO) formed by (**a**) barrier-type and (**b**) porous-type anodizations, along with the respective current (j)–time (t) transients under potentiostatic conditions. This figure by Vicente Neto is licensed under the Creative Commons Attribution 4.0 International https://commons.wikimedia.org/wiki/File: Two_different_types_of_anodic_aluminum_oxide_(AAO).jpg.
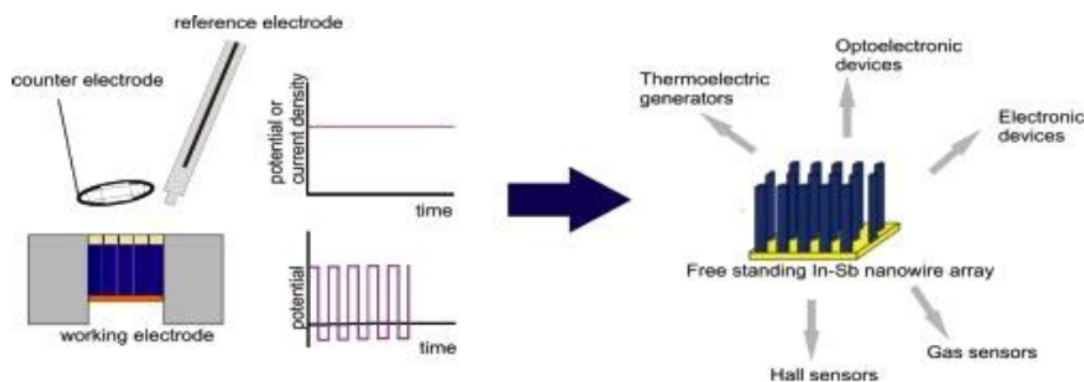
Figure 5: Scheme of the system. Electrochemical methods used to template-assisted fabrication of InSb nanowires. Reproduced with permission from Hnida, K., Mech, J., Sulka, G.D. 2013. Template-assisted electrodeposition of indium–antimony nanowires-Comparison of electrochemical methods Applied Surface Science, 287, 252-256. Copyright (2014) Elsevier B.V. All rights reserved [48].

Indium antimonide (InSb) is a III–V semiconductor compound that in the form of nanowires can improve thermoelectrical and optical properties compared to the corresponding bulk crystal. Hnida *et al*. (20013) [48] applied three electrodeposition (potentiostatic, galvanostatic and periodic pulse reverse) techniques for a fast and inexpensive template-assisted fabrication of InSb nanowire devices from a sodium citrate-citric acid solution at room temperature. Home-made anodic aluminum oxide templates with the pore diameter of 100 nm were used. According to the authors the electrochemical methods used to template-assisted fabrication of InSb nanowires allow controlling their composition and morphology. In the Figure **5** is shown a scheme of this system.

Although electrochemical deposition is widely used for metallic materials deposition, the method is rather occasionally employed for deposition of III–V semiconductor compounds, especially from aqueous solutions. During electrodeposition of semiconductors some challenging tasks have to be overcome, *e.g*. higher resistivity of semiconducting deposit and its sensitivity to crystal lattice defects. These problems are complicated by the fact that resistivity of the deposit can constantly change during electrodeposition. In the Hnida´s work InSb nanowires were electrodeposited from a single bath containing oxidized precursors of both elements using a single potential technique and an unipolar pulse technique with a sequence of on-off cathodic pulses in a two-electrode cell [49, 50]**.** In the Figure **6** is show the In-Sb nanowires obtained by Hnida *et al*. (2013) [37].

Huang *et al*. (2014) [51] working with electrochemical deposition process obtained nanowire
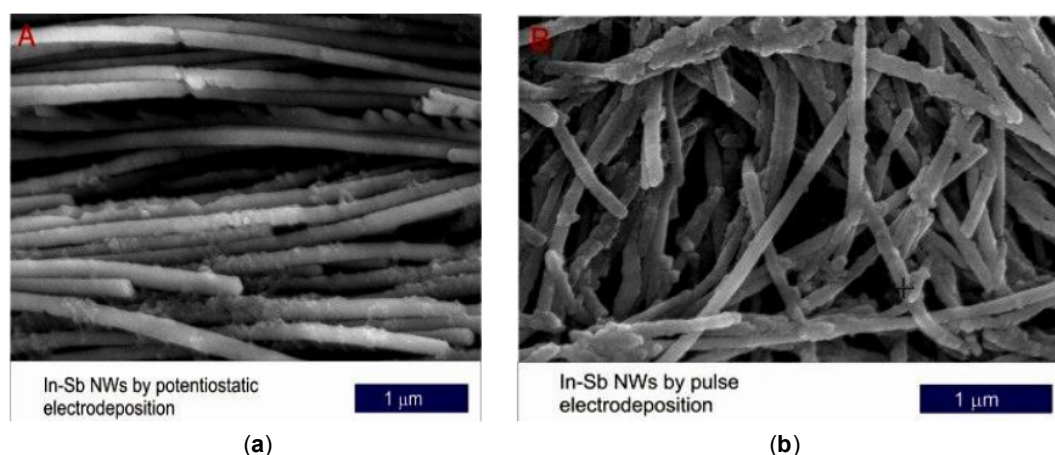
Figure 6: (**a**) In-Sb NWs by potentiostatic electrodeposition, and (**b**) In-Sb NWs by pulse electrodeposition. Reproduced with permission from Hnida, K., Mech, J., Sulka, G.D. 2013.Template-assisted electrodeposition of indium–antimony nanowires Comparison of electrochemical methods Applied Surface Science, 287, 252-256. Copyright (2014) Elsevier B.V. All rights reserved [48].

arrays and to obtain ZnO nanotube the author used anodic alumina oxide template. According to these authors the process of formation of the ZnO nanostructures are described as follows:

$$H_2O_2 + 2e^- \rightarrow 2OH^- \quad E_0 = 0.694V \text{ (vs. SCE)} \tag{1}$$

$$Zn^{2+} + 2OH^- \rightarrow Zn(OH)_2 \tag{2}$$

$$Zn(OH)_2 \rightarrow ZnO + H_2O \tag{3}$$

$$H_2O \rightarrow H_{2g} + O_{2g} \quad E^0 = 1.23V \text{ (vs. SCE)}. \tag{4}$$
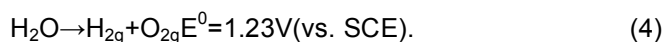
According to Chen *et al*. (2014) [51] as the deposition occurs, H_2O_2 obtains two electrons to form two OH^- (1) at the working electrode. $ZnSO_4$ provides Zn^{2+}, and reacts with OH^- to form the $Zn(OH)_2$ hydrate compound (2). With deposition at 80 °C, $Zn(OH)_2$ is partially dehydrated to nanocrystalline or amorphous ZnO (3) accompanied with hydrogen evolution from electrolysis of water, Eq. (4). The crystallinity increases, and ZnO becomes polycrystalline with annealing at 500 °C in the air. The crystallite size was found to have about 15 nm, calculated by the Scherrer equation. This shows that ZnO was formed and its crystallinity was improved during the dehydration process. It was observed by electron diffraction patterns that ZnO crystalline ring was found in the air, which will be discussed in more detail below. Figure **7** shows a schematic representation of the growth mechanisms of ZnO NT arrays.

The template-assisted electrodeposition can also be used to prepare ordered arrays of 1D nanostructures in the nanochannels of the templates. However, caution must be exercised in the process of removing the templates. Otherwise, it is very easy to destroy the prepared arrays. In order to overcome this disadvantage of the template-assisted electrodeposition, several improved approaches were advanced. Schlenoff used the template-assisted electrodeposition to fabricate ordered arrays of magnetic nanorods with Ni and Au segments [52]. In this patent Ni and Au metals were successively electrodeposited in the nanopores of the AAO membrane which was previously coated with gold on one side Figure (**8a**). After removing the template, the Ni and Au segments of the nanorods were modified with a positively charged polyelectrolyte on Ni or an alkanethiolate on Au to make them either hydrophobic or hydrophilic respectively Figure (**8b**). The modified nanorods were dispersed at the interface of an aqueous phase and a water-immiscible non-aqueous phase. The mutual electrostatic repulsion between each nanorod made them self-assembled into an ordered array Figure (**8c**). Then the nanorods were fixed in the manner depicted in Figure (**8c**) by conversion of the monomers, methyl methacrylate (MMA) in the non-aqueous phase to form PMMA polymer via a polymerization process. Such ordered arrays of the nanorods produced by this method could
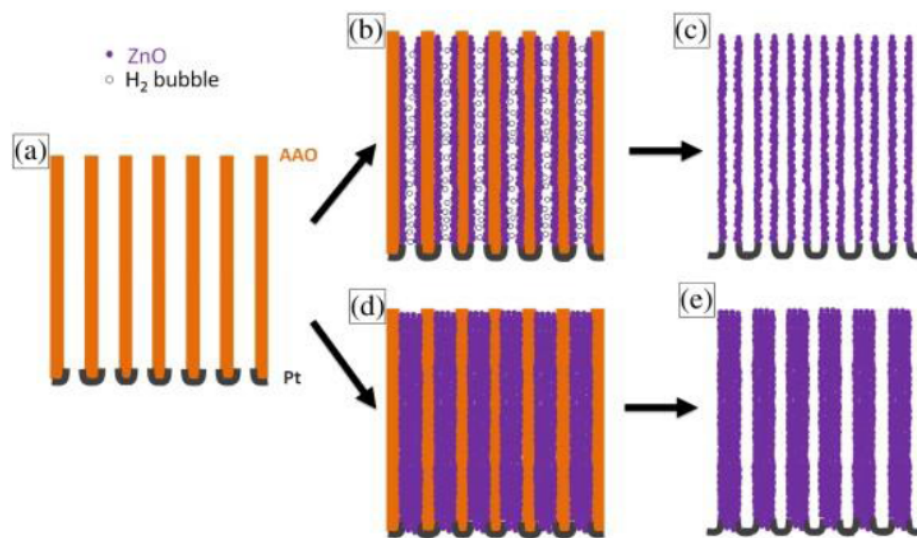
Figure 7: Schematic of the growth mechanisms of (**a**, **b** and **c**) ZnO NT arrays which were deposited in 0.1 M ZnSO4 and 20 vol.% H_2O_2 electrolyte and (**a**, **d** and **e**) ZnO NW arrays which were deposited in 0.5 M ZnSO4 and 20 vol.% H_2O_2 electrolyte via the AAO template-based electrochemical deposition method [51]. Reproduced with permission from Chen, Y.-H.; Shen, Y.-M.; Wang, S.-C. & Huang, J.-L. (2014). Fabrication of one-dimensional ZnO nanotube and nanowire arrays with an anodic alumina oxide template via electrochemical deposition, Thin Solid Films 570, Part B, 303–309, ISSN: 0040-6090. Copyright (2014) Elsevier B.V. All rights reserved.
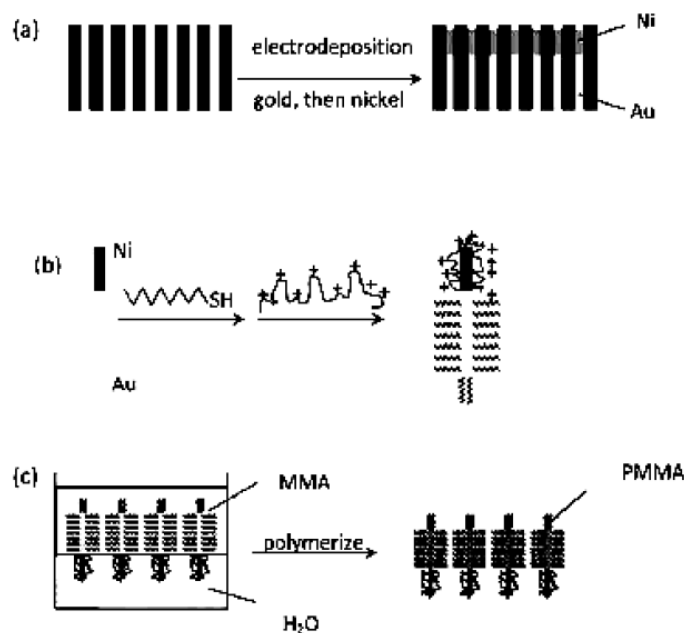
Figure 8: Schematic diagrams illustrating the ordered arrays of nanorods fabrication process. Reproduced with permission from [53] (Figure 3 from Recent Patents on Nanotechnology 2009, 3, 182-191).

have great potential in ultra-high density magnetic storage and other applications.

2.1.2.3. Step Edges

The step-edge template assisted synthesis of 1D nanostructures was pioneered by Himpsel [54, 55] and Kern *et al*. [56, 57]. Step edges on a surface can be used as another kind of templates for preparing supported 1D nanostructures.

The exposed edges of steps within a crystalline lattice can have properties that are different from those of the bulk material. For example, gas-phase catalytic studies have shown that the exposed edges of the catalyst can promote a number of reactions and are often the sites of highest reactivity [58, 59]. The step edges on single-crystalline surfaces can also direct the growth of metal nanostructures [60-63]. Penner and coworkers developed this method to electrodepositing nanowires with controlled diameters of metals and metal oxides [64]. Menke and Penner, 2004 [65] synthesized bismuth telluride (Bi_2Te_3) nanowires by Cyclic Electrodeposition/ Stripping coupled with Step Edge Decoration. This material is a particular thermoelectric material for power generation. They are members of the $Bi_{2(1-x)}Sb_{2x}Te_{3(1-y)}Se_{3y}$ family. In the work [65] polycrystalline bismuth telluride (Bi_2Te_3) nanowires was prepared by the step edge selective electrodeposition of Bi_2Te_3 on highly oriented pyrolytic graphite (HOPG) surfaces. Bi_2Te_3 nanowires were
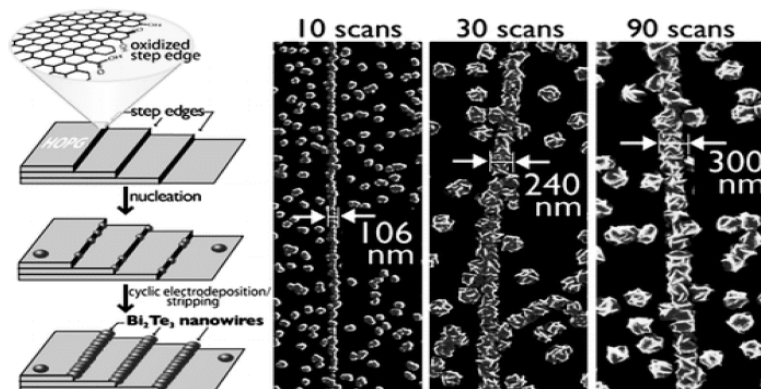
Figure 9: Schematic diagram of the three-step method employed for synthesizing Bi_2Te_3 nanowires by cyclic electrodeposition/stripping coupled with ESED [65] Reprinted with permission from Menke, E. J.; Li, Q. & Penner, R. M. (2004). Bismuth telluride (Bi2Te3) nanowires synthesized by cyclic electrodeposition/stripping coupled with step edge decoration," Nano Lett. 4, 2009–2014, ISSN: 1530-6992.). Copyright (2004) American Chemical Society. All rights reserved.

obtained from an aqueous plating solution containing Bi^{3+} and $HTeO_2^+$. Figure **9** shows the schematic diagram of the method employed for synthesizing Bi_2Te_3 nanowires.

The stepped surface is energetically favourable for an electrochemical formed atom to attach itself to the defect sites, such as the surface step edges [66]. Particles of Cu, Co, and Ag have been deposited at the step edges of crystalline metallic substrates (*e.g.*, Mo (110), Ag (111), and Cu (111)) [67, 68]. These metals are often deposited by physical vapour deposition.

Material deposition at atomic step edges has been extended to the growth of continuous nanowires by electrodeposition on highly oriented pyrolytic graphite (HOPG) (Figure **10 a-c**).

This kind of approach can generate nanowires of metals (*e.g.*, Ag, Pd, Cu, and Au), oxides (*e.g.*, MoO_x and Cu_2O), and semiconductors (*e.g.*, MoS_2 and MnO_2, Figure **11**) [70, 71].

These nanowires can have lateral dimensions as small as ~ 15 nm having application in the fabrication of
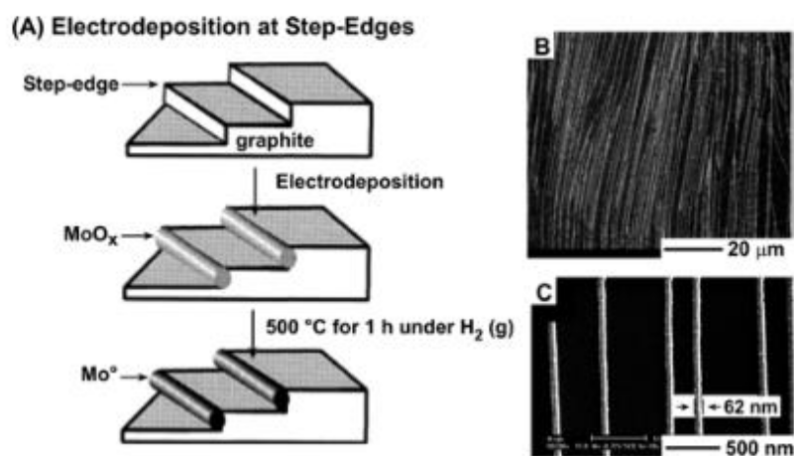
Figure 10: (A) Schematic illustration of the process used to generate nanowires at step edges of a graphite surface by electrodeposition of a material such as molybdenum oxide (MoOx). SEM images (B, C) show dense arrays of MoOx nanowires deposited from 1.0 mM MoO_4^{2-}.[69] Reprinted (adapted) with permission from Gates, B. D.; Xu, Q.; Stewart, M.; Ryan, D.; Willson, C. G. & Whitesides, G. M. (2005). "New Approaches to Nanofabrication: Molding, Printing, and Other Techniques," Chemical Reviews 105(4), 1171–1196, ISSN: 1520-6890. Copyright (2005) American Chemical Society. All rights reserved.
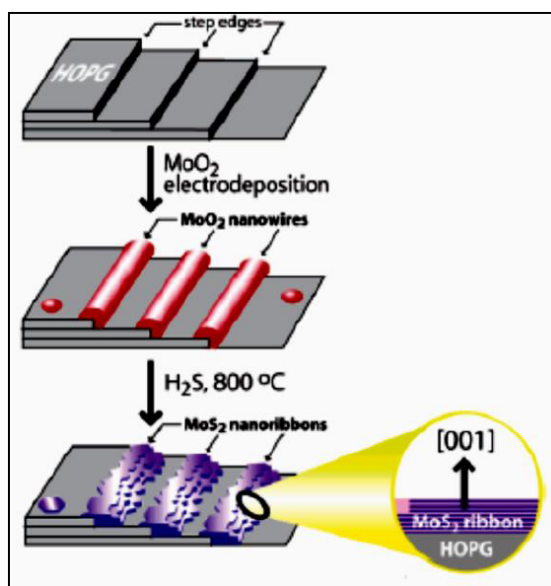
Figure 11: The E/C (Electrochemical/Chemical Synthesis) method for synthesizing 2H−MoS_2 nanoribbons on graphite surfaces [70]. Reprinted with permission from Li, Q.; Newberg, J. T.; Walter, E. C.; Hemminger, J. C. & Penner, R. M. (2004). Polycrystalline Molybdenum Disulfide (2H−MoS2) Nano- and Microribbons by Electrochemical/Chemical Synthesis," Nano Lett. 4(2), 277–281, ISSN: 1530-6992.. Copyright (2004) American Chemical Society. All rights reserved.
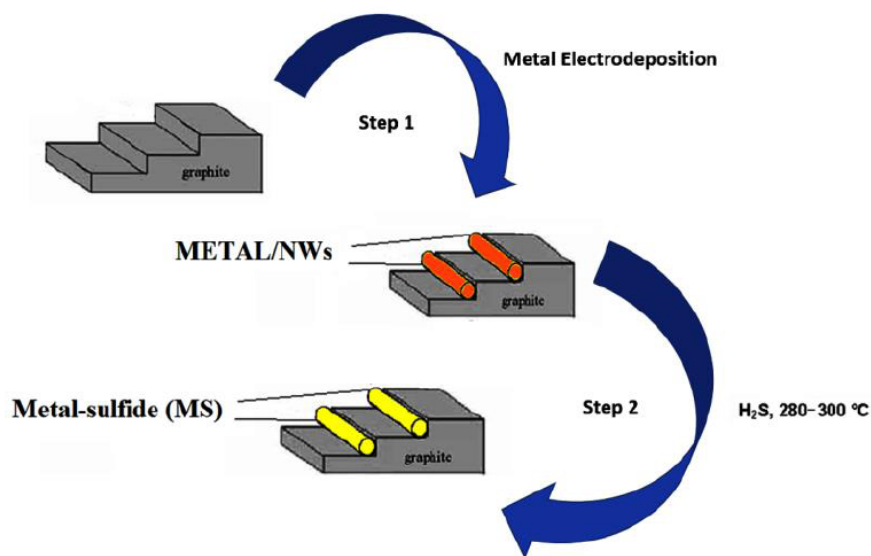
Figure 12: Schematic diagrams illustrating Step-edge template-assisted synthesis of 1D nanostructures. This file is licensed by Vicente Neto under the Creative Commons Attribution 4.0 International license. Link: https://commons.wikimedia.org/wiki/File:Schematic_diagrams_illustrating_Step-edge_template_assisted_synthesis_of_1D_nanostructures.tif.

gas sensors. For example, palladium nanowires, transferred to a cyanoacrylate polymer film, can be used to detect the presence of hydrogen gas [72]. Nanowires grown by this method are, however, randomly positioned on the substrate in a pattern determined by the orientation and spacing of the step edges in the HOPG substrate. Their grain structures and edge roughness were not characterized. The diameter of these stated compounds can also vary across the substrate, and nanoparticles can nucleate on defects in the substrate. Figure **12** shows Schematic diagrams illustrating step-edge template-assisted synthesis of 1D nanostructures.

2.1.2.4. Polymer Membrane

In the 1960s, Price and co-workers, from General Electric Research Laboratory, Schenectady, New York, discovered that the damage tracks produced in mica by high energy particles could be preferentially etched to yield pores. The diameters of the pores were dependent on the etching time [73, 74]. With the progress of the science this procedure for etching damage tracks was further improved to be used in other minerals and polymers [75]. The track-etched polymer membranes have been proven to be especially useful as another kind of template materials for electrodeposition of 1D nanostructure. Chien *et al*. used the polycarbonate membrane as template to fabricate arrays of Bi nanowires via electrodeposition [76]. Sager *et al*. described a process for fabricating a

solar cell comprising oriented arrays of semiconducting nanostructures in conducting or semiconducting polymeric materials [77]. The template strategy combined with electrodeposition techniques have been successfully used to produce nanoscale objects in the cylindrical pores of track-etched polycarbonate membranes.

Using this method, nanometer-size metallic wires, conductive polymer nanotubules, superconducting nanowires and quasi-one-dimensional magnetic multilayers have been fabricated. When restricted to the field of materials sciences, the main interest is that the physical properties of a material can change in the transition between the bulk scale and the nanoscale. In fact these nanoscale materials exhibit physical properties different from those found in the bulk. Martin ([78] 1996) and his research group developed an experimental procedure called Template method (Figure **13**). In this method metals can be deposited within the pores of the template membranes by either electrochemical or chemical ("electroless") reduction of the appropriate metal ion. Electrochemical deposition is accomplished by simply coating one face of the membrane with a metal film and using this metal film as a cathode for electroplating [79-81].

In general, this method is only applicable to electrically conductive materials such as metals, alloys, semiconductors, and electrically conductive polymers
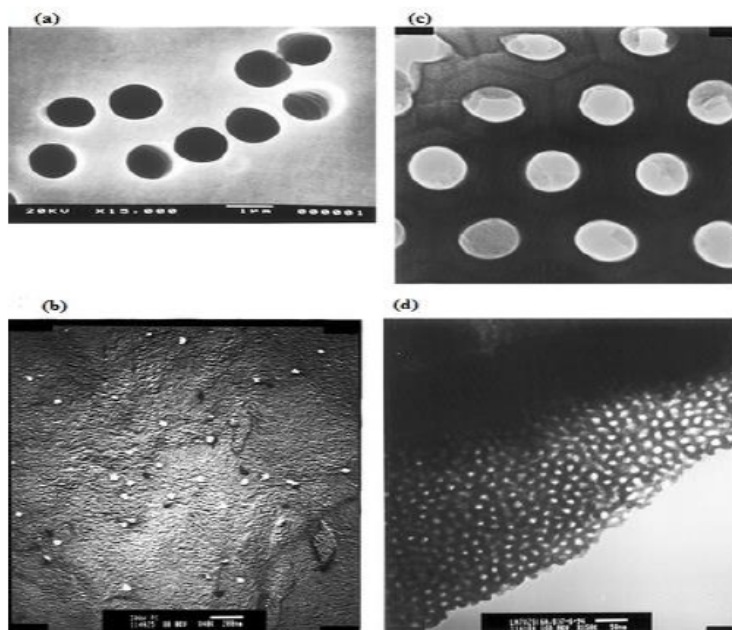
Figure 13: Electron micrographs of polycarbonate (**a** and **b**) and alumina (**c** and **d**) template membranes. [78]. Reprinted with permission from Martin, C. R. (1996). "Membrane-Based Synthesis of Nanomaterials," Chem. Mater. 8(8), 1739–1746, ISSN: 1520-5002.

(Figure **14**). After the initial deposition, the electrode is separated from the depositing solution by the deposit and so the deposit must conduct in order to allow continuation of the deposition process. When the deposition is confined to the pores of the plate membranes, nanocomposites are produced. If the template membrane is removed, nanorod or nanowire arrays are prepared.

It is generally accepted that the template-assisted electrodeposition provides a simple, high throughput and cost effective procedure for the fabrication of 1D nanostructures. The advantages of template-assisted electrodeposition include: (a) a general approach for almost all materials; (b) batch fabrication ability; (c) accurate control of the diameter and length of the 1D

nanostructures through controlled pore growth and time of growth; (d) control of composition through the electrolyte and electrodeposition parameters. However, the template-assisted electrodeposition has some serious limitations, such as (i) required a post treatment process to remove the template, (ii) the nanostructures obtained are often polycrystalline and (iii) the quantity of the nanostructures that can be obtained in each run of the synthesis is limited.

3. TEMPLATE-FREE ELECTRODEPOSITION: ALTERNATIVE TECHNIQUES

3.1. Template-Free Electrodeposition

To generate 1D morphologies, templates are often used during the electrodeposition process (template-
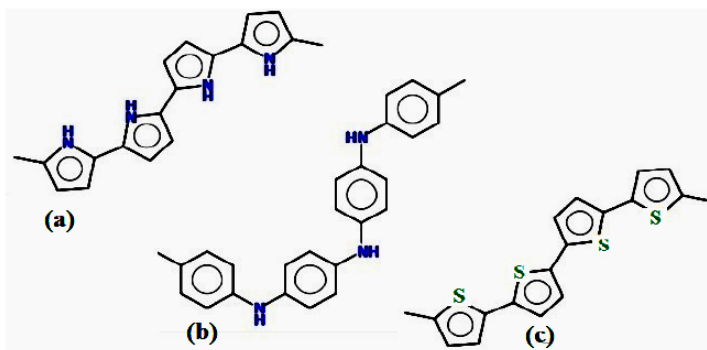
Figure 14: Some electronically conductive polymers. (a) Polypyrrole; (b) Polyaniline. and (c) Polythiophene.

assisted electrodeposition, TAED) [82, 83]. This method has been widely used to prepare 1D nanostructures of many materials [14]. By using a template, nanorods and nanotubes with uniform diameters as well as segmented nanorods can be readily grown in an array [84, 85]. According to experimental evidence it is known that some materials attain 1D growth under certain conditions without using any template due to their intrinsic highly anisotropic crystal structures [86], as occurs with CdSe nanowires on conducting glass [87]. Feng *et al*, describe a low-temperature and directed preparation of CdSe nanowires in a simple one-step, template-free electrochemical deposition. According to them with the discovery of other one-dimensional CdSe nanostructures and CdS nanowires, it is anticipated that the electrochemical synthesis method can be extended to other nanostructures of CdSe and to other II−VI semiconductors and also be used to develop a systematic synthesis for nanostructured semiconductors. The average diameter of the thus prepared CdSe (by TFED method) nanowires was larger than those synthesized by chemical vapor deposition (CVD) and solution−liquid−solid (SLS) methods (Figure **15**).

The electrochemical reaction process can be simply expressed as eq 5:

$$Se(s) + 2e^- \longrightarrow Se^{2-}(aq) \qquad (5)$$
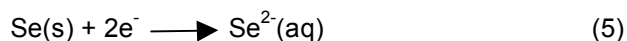
Elemental Se was reduced to Se^{2-}, and then CdSe was formed as a result of the electrostatic attraction:

$$Cd^{2+}(aq) + Se^{2-}(aq) \longrightarrow CdSe\ (s) \qquad (6)$$

In the the Zhou *et al.* work the electrodeposition conditions included the bath temperature, the current density, the stirring rate, and the concentrations of the reactants, which were varied to generate the CdSe nanowires. In the next step, a current density of 0.22 mA cm^{-2}, a temperature of 147 °C, a concentration of 10 mM for $CdCl_2$ and 5 mM for elemental Se, and a stirring rate of 1000 revolutions per minute (rpm) were used as the typical electrodeposition conditions to make the CdSe nanowires. After deposition, CdSe nanowire samples were sequentially cleaned in acetone and ultrapure water and then annealed at 350 °C under inert gas (N_2) shielding for 60 min to acquire the better photovoltaic performance [88]. Applications of CdSe nanowires have previously focused on light-emitting diodes (LEDs), optoelectronic devices, and field-effect transistors (FETs) [89] because of their direct band gap (~ 1.74 eV at room temperature), good visible-light absorption, and excellent photoelectrical characteristics [90, 91].

Other interesting material is CuTe nanoribbons [92]. It has been synthesized by template-free electrodeposition (TFED) based on the intrinsic anisotropic structures. Copper telluride (CuTe) is a transition metal chalcogenide with interesting electronic
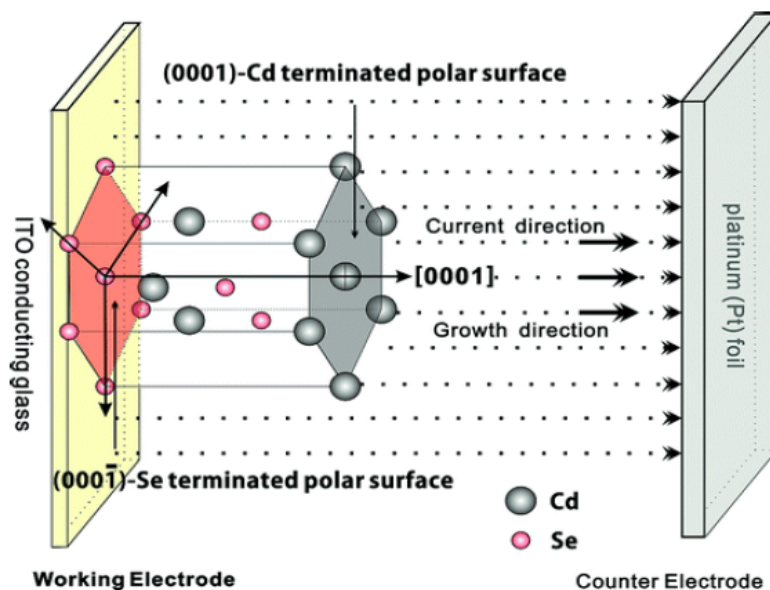
Figure 15: Schematic diagram of the wurtzite structure and the proposed electrodeposition process of the CdSe nanowires. Reprinted with permission from Feng, Z.; Zhang, Q.; Lin, L.; Guo, H.; Zhou, J. & Lin, Z. (2010). ⟨0001⟩-Preferential Growth of CdSe Nanowires on Conducting Glass: Template-Free Electrodeposition and Application in Photovoltaics, Chem. Mater. 22(9), 2705–2710, Copyright (2010) American Chemical Society. All rights reserved.

and photoelectric properties and potential applications. A template-free electrochemical deposition method was successfully used to synthesize single-crystal CuTe nanoribbons (Figure **16**) in the temperature condition with usage of aqueous solution [93]. It was suggested that the ribbon-like morphology of the CuTe resulted from the synergistic effect of the anisotropic crystal structure of the CuTe and thermodynamics of the crystal growth process. In this study, CuTe nanoribbons were synthesized for the first time by an electrochemical method from an aqueous solution at 85 °C without using any template or capping agent. This technique was developed by Shi *et al*. (2008). They applied TFED to synthesize 1D nanostructures of Te and CuTe [93a,93b, 94]. In that work TeO_2 or tellurate dissolved in an alkaline solution (such as KOH) was used as electrolyte. It is therefore expected that under proper conditions, TFED could be employed as a versatile method for synthesizing various 1D materials which contain intrinsic highly anisotropic crystal structures.

Algarni *et al*. 2018 [93b] reported on a strategy to grow *a*-InSb (*a*, amorphous) NWs in the CVD system (Figure **17**). According to the authors, the lack of crystallinity in the as-grown NWs can be attributed to the effect of post-growth annealing treatment on the electronic and optical quality of the a-InSb NWs.

3.2. Other Templates

In aqueous solution, surfactant molecules aggregate into micelles and further into lyotropic liquid-crystalline phases at higher concentrations. The lyotropic mesophases are categorized into three major types: hexagonal phases (H1), cubic phases (Ia3d) and lamellar phases (Lα) [95]. Hexagonal phases consist of aligned cylindrical micelles in a hexagonal array. In cubic phases they are interconnected on a gyroid lattice and the lamellar phases consist of lamellar structured micelles. The hexagonal phases of lyotropic liquid crystals have been employed as templates for electrosynthesis to form hexagonally mesoporous materials [96-99]. Shin *et al*. [100] developed hydrogen bubbles as a novel template to create mesoporous structures via electrochemical routes. Vigorous hydrogen evolution occurs when a large negative current is applied in an acidic electroplating solution. The hydrogen bubbles produce a continuous path from the electrode surface to the electrolyte–air interface and act as a template to form foam structures. Xu *et al*. [101] have produced polymer templates exhibiting a uniform porous structure that is the inverse of an opal. The templates were fabricated by performing polymerization in the voids of pre-formed silica colloidal crystals and removing silica after filling the voids.

Riley *et al*. [102] employed the polymer membranes with a negative structure of sea urchin plates as templates for electrodeposition of porous materials. The polymer membrane was synthesized by polymerization within the original sea urchin plates and subsequent dissolution of inorganic plates.

4. ENVIRONMENTAL PERSPECTIVES: CLEAN METHOD
4.1. La(OH)$_3$ and La$_2$O$_3$ as Nanotubes

The syntheses of the nanomaterial with one or two-dimensional (1D or 2D) can be prepared by the usage

(a)   (b)
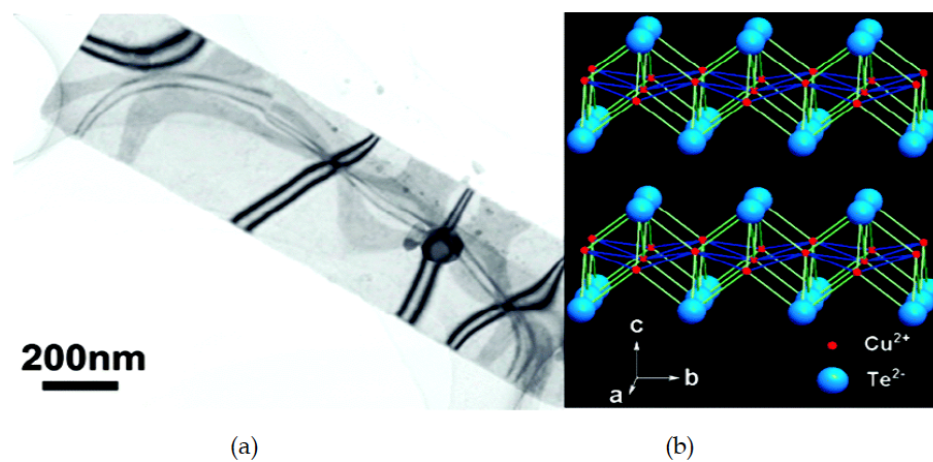
Figure 16: (**a**) TEM image of the nanoribbon and its corresponding structural model of the layered CuTe crystal. Reprinted with permission from She, G.; Zhang, X.; Shi, W.; Cai, Y.; Wang, N.; Liu, P. & Chen, D. (2008). "Template-Free Electrochemical Synthesis of Single-Crystal CuTe Nanoribbons," Crystal Growth & Design 8(6), 1789–1791. Copyright (2004) American Chemical Society. All rights reserved.
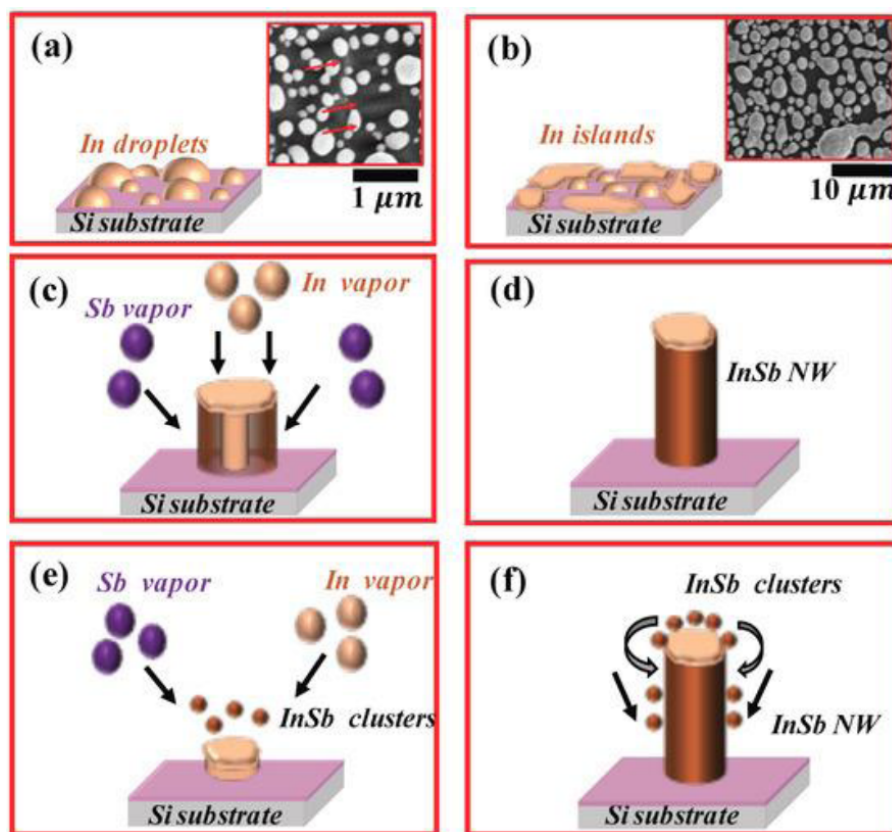
Figure 17: Schematic of the two possible growth mechanism of a-InSb NWs. (**a**) Initiation of NW growth as a result of In droplets forming on the Si substrate. These droplets have different sizes as shown in the inset; (**b**) As temperature rises at a very high rate, the droplets coalesce into islands and migrate to the edge of the Si substrate. Smaller In droplets are left behind at the center of the Si substrate; inset shows In islands coalescing and ripening; (**c,d**) Possible growth mechanism 1, in which an In core first precipitates from the molten seed (**c**), followed by complete antimonidization of the In core, resulting in an InSb NW (**d**); (**e,f**) Possible growth mechanism 2, in which In and Sb atoms combine to form InSb clusters over the molten In droplet (**e**). These clusters settle on the surface of the molten droplet and slips to the lower hemisphere and diffuses to the interface between the substrate and the molten In droplet (**f**). The mechanisms follow those reported for the growth of a-SiOx NWs.

of $La(OH)_3$ and La_2O_3 compounds through the electrochemical deposition method. For instance, nanorods, nanotubes, nanowires, nanocapsules and nanoplates [103-109] can be prepared by this important method. The syntheses of this stated nanomaterial is very important since this material present many application in technological fields such as hydrogen storage for the fuel cell technology, light-emitting phosphor, electrode for the electronic device, high potential oxides, catalyst in the chemical reaction, automobile exhaust-gas convector and sorbent materials for the environmental problems [110-113]. The synthesis nanospindles and nanorods based on of $La(OH)_3$ compound was prepared by Lui *et al*. (2010) through the galvanostatic deposition (i = 1 mA cm^{-2}) on the surface of F-doped SnO_2 substrates from 0.01 M $La(NO3)_3$+50% DMSO at temperature of 70 °C for 60 min in a bath [114]. The stated spindle-like nanostructures was prepared with $La(OH)_3$ compound and was reported for the first time by Aghazadeh *et al.* [115]. The nanostructure material is prepared by the

deposition process on the surface of the stainless steel substrate using aqueous solution with a concentration of 0.005 M $La(NO_3)_3$. Continuous the process it is applied a density of current of 2 mA cm^{-2} during 25 min at 60 °C. Following a heat treatment is applied in the hydroxide nanospindles at 600 °C for 3 h to produced the La_2O_3 nanospindles.

The Figure **18** show the process of formation of $La(OH)_3$ that occurring through deposition on the cathode. In the works cited above it was proposed the mechanism below:

Electrochemical step

$$2H_2O+2e^-\rightarrow H_2+2OH^- \quad E°=-1.08 \text{ V vs. Ag/AgCl} \quad (7)$$

Chemical step

$$La^{3+}(aq)+3OH^-(aq)+xNO^-_3+yH_2O\rightarrow[LaM(OH)_{(3-x)}(NO_3)_x \times yH_2O]\downarrow \quad (8)$$
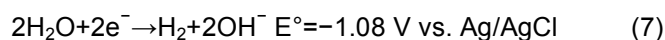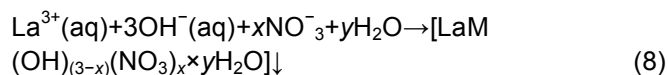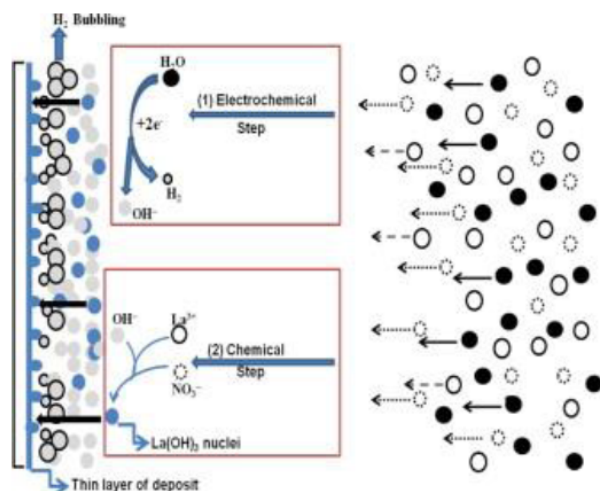
Figure 18: A schematic view of the La(OH)₃ deposition from nitrate bath. Reproduced with permission from Aghazadeh, M.; Arhami, B.; Barmi, A.-A. M.; Hosseinifard, M.; Gharailou, D. & Fathollahi, F. (2014). "La(OH)3 and La2O3 nanospindles prepared by template-free direct electrodeposition followed by heat-treatment, Mat. Lett. 115, 68–71 [115]. Copyright (2014) Elsevier B.V. All rights reserved.

Recording the potential values during the deposition time (−1.09 V vs. Ag/AgCl) Aghazadeh *et al*. [116] observed that the water reduction has the major role in the base electrogeneration. Remarkably, the strings of gas bubbles were experimentally observed on the cathode surface during all times of deposition confirming the water reduction during the electrochemical step (7). In the same work Aghazadeh *et al*. [116] have investigated the thermal behavior (DSC-TG) of the lanthanum hydroxide powder and the main results are shown in Figure **19**. In the DSC curve,

four endothermic peaks are seen, corresponding to the following steps:

(i) Removal of the physically adsorbed water below 200 C

$$[La(OH)_{(3-x)}(NO_3)_x \times yH_2O] \rightarrow [La(OH)_{(3-x)}(NO_3)_x] + yH_2O$$

$$(9)$$
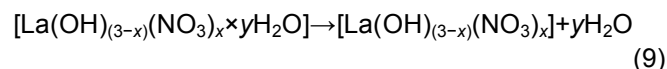
(ii) Removal of the structural water between 200 and 390 °C

$$[La(OH)_{(3-x)}(NO_3)_x] \rightarrow [LaO(OH)_{(1-x)}(NO_3)_x] + (2-x)H_2O$$

$$(10)$$
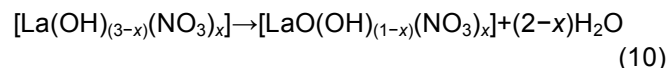
(iii) Removal of the residual structural water between 390 and 450 °C

$$[LaO(OH)_{(1-x)}(NO_3)_x] \rightarrow 2LaO(NO_3)_x + (1-x)H_2O \qquad (11)$$

(iv) Removal of the intercalated nitrate ions at 450 and 600 °C

$$LaO(NO3)_x \rightarrow La_2O_3 + 2xNO_2 + x/2O_2 \qquad (12)$$
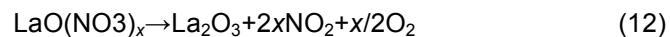
According to the thermogravimetric analysis (DSC-TGA) the total weight loss of the hydroxide sample is 13.5 wt%. Approximately 3.9 wt% of the total amount of weight loss corresponds to the physically adsorbed water (9). The weight losses of ~6.5 wt% is also due the elimination of the structural water (10) and ~1.6 wt% of total weight loss is related to the removal of the residual structural water (11). The last weight loss of 1.5 wt% can be assigned to the removal of intercalated
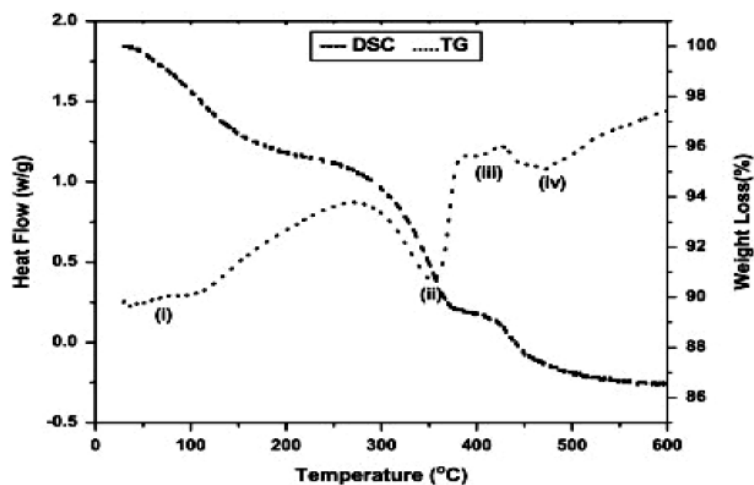
Figure 19: Thermogravimetric analysis (DSC-TGA) of the La(OH)3 nanospindles. Reproduced with permission from Aghazadeh, M.; Arhami, B.; Barmi, A.-A. M.; Hosseinifard, M.; Gharailou, D. & Fathollahi, F. (2014). "La(OH)₃ and La₂O₃ nanospindles prepared by template-free direct electrodeposition followed by heat-treatment, Mat. Lett. 115, 68–71 [115]. Copyright (2014) Elsevier B.V. All rights reserved.
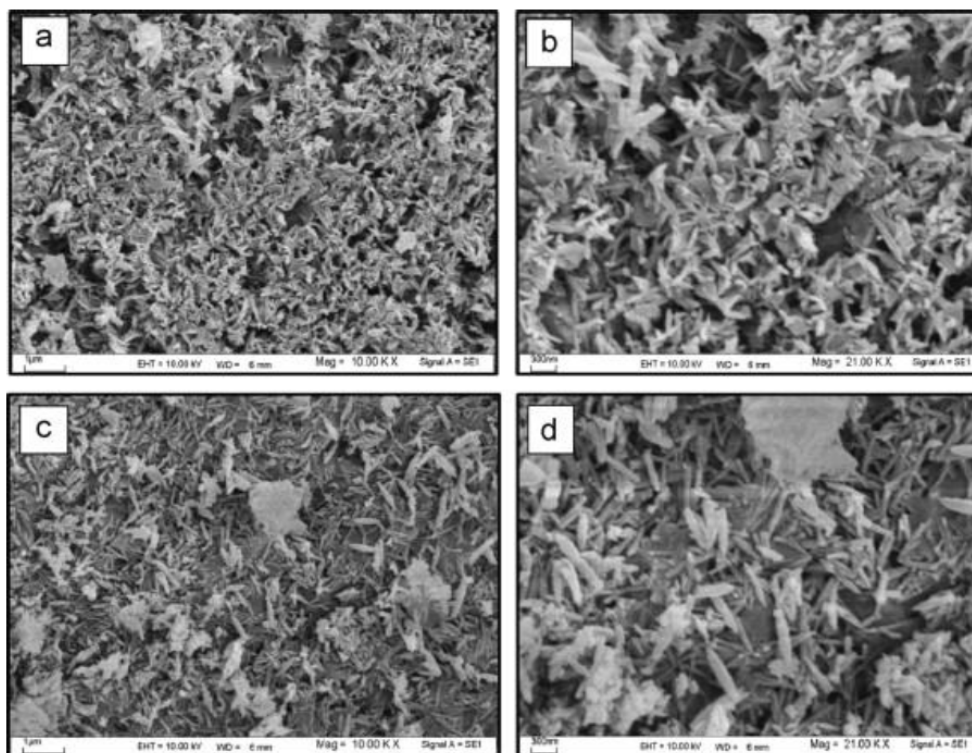
Figure 20: SEM images of the prepared La(OH)$_3$ (**a**) and (**b**) and La$_2$O$_3$ (**c**) and (**d**) nanospindles. Reproduced with permission from Aghazadeh, M.; Arhami, B.; Barmi, A.-A. M.; Hosseinifard, M.; Gharailou, D. & Fathollahi, F. (2014). "La(OH)$_3$ and La$_2$O$_3$ nanospindles prepared by template-free direct electrodeposition followed by heat-treatment, Mat. Lett. 115, 68–71 [115]. Copyright (2014) Elsevier B.V. All rights reserved.

nitrate ions (12). Figure **20** shows morphological characteristics of products through SEM measurements.

4.2. One Dimensional-ZnO

4.2.1. One Dimensional-ZnO Nanostructures: Dyes and Organic Chemicals Removing

An enormous amount of dyes and organic chemicals produced by industrial processes are discharged into the environment on a daily basis. The presence of these contaminants in water causes considerable problems to microorganisms, aquatic environments and human beings [116-118]. About 10–15% of the total world production of dyes is lost during the production process and is released in the textile effluent [119, 120]. The discharge of these colored, contaminated wastewaters into the environment represents a considerable source of non-aesthetic pollution and eutrophication and could create dangerous byproducts through oxidation, hydrolysis, or other chemical reactions occurring in the wastewater stream [121].

According to Forgacs *et al*. [122] traditional wastewater treatment technologies have proven to be mostly ineffective for removing synthetic textile dyes from wastewater because of the chemical stability of these pollutants; they also verified that 11 out of 18 azo dyes selected for their investigation passed through the activated sludge process practically untreated. Most textile dyes are stable towards chemical oxidation [123-125]. These characteristics render them resistant towards decomposition by conventional biochemical and physico-chemical methods. To summarize, the aforementioned processes have wide-ranging limitations in efficacy for the removal of dyes from waste-water.

ZnO has been investigated by researchers due to its higher photoactivity (by a factor of 2–3) in both UV and sunlight irradiation for the decontamination of water [126, 127]. Beyond that, due to ZnO higher efficiency in the production of OH· and reduced recombination of photoinduced electron–hole pairs, it has been considered to be more photoactive [128, 129]. Generally, the surface area and the number of defects on the surface of the catalyst are significant parameters for the effective photochemical reaction. Although nanoparticles offer a larger surface area, they are limited in their use in a water suspension because of the difficulty and high cost of separation and

recovery. One dimensional nanostrutures, such as NWs and NRs, offer enhanced photocatalytic efficiency [130-132], and could be well alligned on most surfaces with no post-treatment of the catalyst. A comparison of various ZnO nanostrutures for photocatalytic applications is presented in Table 1. As illustrated, 1D-nanostructures, such as NWs, NRs and nanotubes, provide higher surface area to volume ratio compared to nanoparticles [133] in thin films (two-dimensional nanostructures). Among the 1D-nanostructures, ZnO NRs and NWs have been widely studied because of their nanomaterial formation and device applications.

4.2.2. ZnO and Solar Cells

Dye-sensitized solar cells (DSSCs) have been regarded as promising devices for energy applications because of their advantages of low cost, ease of manufacture, and use of low toxicity materials [134-137]. The photoelectrode in DSSC (Figure **21**), which is based on mesoporous wide-band gap semiconductor nanocrystalline films sensitized by a monolayer of dye molecules, represents the heart of the device.
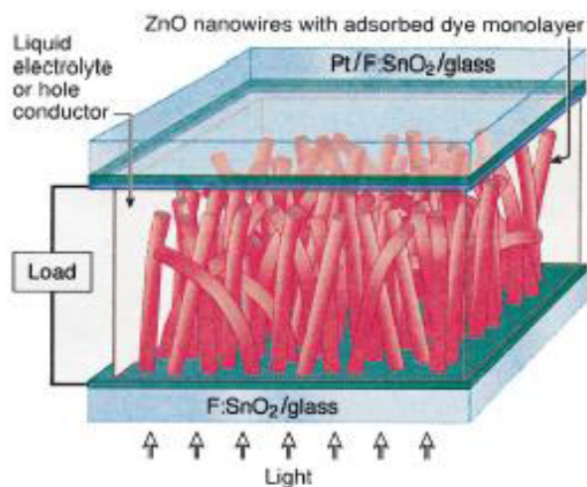
Figure 21: A DSSC device using ZnO nanowires, enabling a high surface area while minimizing the number of grain boundaries that must be crossed by photogenerated charges. Reproduced with permission from Baxter, J. B. & Aydil, E. S. (2005). Nanowire-based dye-sensitized solar cells, Appl. Phys. Lett. 86(5), 053114. Copyright (2005) AIP Publishing. All rights reserved.

A very important feature provided by the mesoporous nanocrystalline films is the high internal surface area (1000–2000 times the area of a flat/smooth electrode), which ensures sufficient dye loading for the photoelectrode and thus good light harvesting efficiency for the cell (Figure **22**). It has been demonstrated that the trap-detrap diffusion process of electron transport in mesoporous nanocrystalline film, mainly caused by the defects in the nanocrystalline film, is a major limiting factor for achieving higher power conversion efficiency [138, 139]. Replacing the mesoporous nanocrystalline films with one-dimensional (1D) zinc oxide (ZnO) nanostructures, such as nanowire arrays [140] or nanotube arrays [141] is considered to be an effective way to tackle this issue. This occurs not only because 1D ZnO nanostructures can afford a direct conduction pathway for the photogenerated electron, but also because they exhibit much more higher electronic mobility (200–1000 cm^2 V^{-1} s^{-1}) than TiO_2 nanostructures (0.1–4.0 cm^2 V^{-1} s^{-1}), which would be favorable for rapid electron transport in photoelectrode with reduced recombination loss [12-14, 142, 143]. The power conversion efficiencies of the 1D ZnO nanostructure-based devices, however, are restricted to a relatively low level by the low light harvesting efficiency, which is the result of low internal surface area provided by 1D nanostructure photoelectrodes. Thereby hierarchical ZnO nanostructures combining multiscale configurations, such as tetrapod-like nanostructures [144], nanoflower structures [18, 145] dendritic nanowires [15, 16, 146] and nanowire-nanosheet architectures [147] are introduced, aimed at enlarging internal surface area of the photoelectrode while keeping high electron transport efficiency.
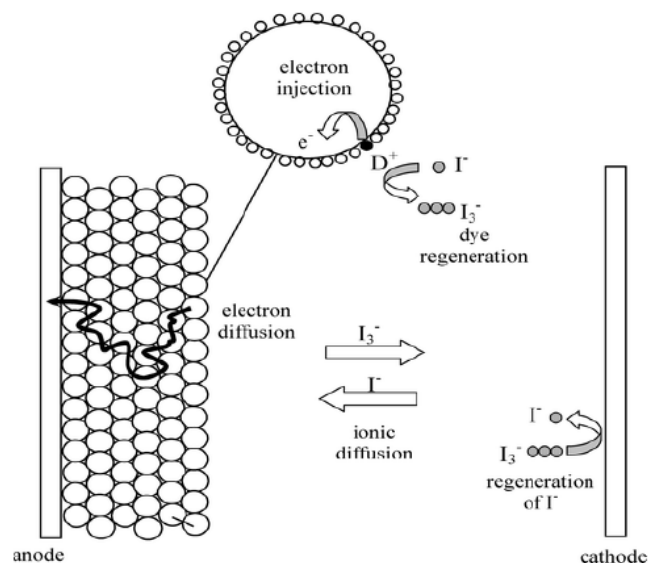
Figure 22: Summary of the key processes involved in the regenerative cycle taking place in a dye-sensitized solar cell under illumination Reproduced with permission from Peter, L. M. (2007). "Characterization and Modeling of Dye-Sensitized Solar Cells," J. Physical Chemistry C 111(18), 6601–6612. Copyright (2007) American Chemical Society. All rights reserved.

Electrodeposition of ZnO nanostructures is generally based on the generation of OH– ions at the surface of working electrode by electrochemical

reduction of precursors such as O_2,(13) NO_3^-,(14) and H_2O_2(15) in Zn^{2+} aqueous solution [148-150]. During the deposition process, OH^- ions are produced in terms of (13), (14), or (15) after certain potential is applied. Then Zn^{2+} ions in the vicinity of working electrode react with OH^- ions, resulting in formation of zinc hydroxide $(Zn(OH)_2)$ (eq 16). Finally, ZnO is produced by dehydration of $Zn(OH)_2$ (17).

$$O_2 + 2H_2O + 4e^- \; 4OH^- \tag{13};$$

$$NO_3^- + H_2O + 2e^- \; NO_2^- + 2OH^- \tag{14}$$

$$H_2O + 2e^- \; 2OH^- \tag{15}$$

$$Zn^{2+} + 2OH^- \rightarrow Zn(OH)_2 \tag{16}$$

$$Zn(OH)_2 \rightarrow ZnO + H_2O \tag{17}$$

The morphology of the as-synthesized ZnO nanodeposits strongly depends on the experimental conditions, particularly the Zn^{2+} concentration, which might change the reaction rate of the hydroxylation (16) and dehydration (17), thereby enabling modifying the growth behavior of ZnO nanodeposits [149, 150]. In the Figure **23** is shown the growth of ZnO nanostructures on ITO-glass. In the same scheme is possible to see the growth behavior of ZnO nanostructure 1D and 2D. In the electrolyte containing a low concentration of Zn^{2+}, the dehydration reaction is faster than the hydroxylation one. Thus, $Zn(OH)_2$ can be converted into ZnO as soon as it is produced, leading to formation of 1D ZnO nanostructures (*e.g.*, nanorods, nanowires, or nanopillars) because of the anisotropic growth along the [0001] direction of the hexagonal wurtzite structure. However, the formation of ZnO produced by dehydration of $Zn(OH)_2$ could be delayed because of

the relatively faster hydroxylation reaction in the case of high Zn^{2+} concentration. As a result, the growth along [0001] direction might be replaced by other preferred growth direction, such as [01$\bar{1}$0] or [10$\bar{1}$0], which can give rise to formation of 2D nanostructures (*e.g.*, nanosheets or nanowalls). Accordingly, hierarchical ZnO nanostructures could be obtained by designing a multistep electrodeposition process (Figure **23**), in which the Zn^{2+} concentrations in different steps are adjusted in order to obtain ZnO nanodeposits with desired morphologies.

4.2.3. One Dimensional-TiO$_2$ Nanostructures: Dyes and Organic Chemicals Removing

The multi-functionality of semiconducting titanium dioxide (TiO_2) has seen its utilization in numerous industrial applications. Known largely for its strong photocatalytic activity, robust chemical stability under acidic and oxidative environments, low production cost and non-toxicity, TiO_2 has found uses in areas such as photocatalysis [152, 153] and dye-sensitized solar cells [154]. Amongst a myriad of existing TiO_2 structures, highly ordered one-dimensional (1D) nanostructures, formed by anodization of Ti [155] or electrodeposition from solutions containing $TiCl_3$ as a precursor [156], have been found to be particularly important in achieving scalable functional devices. A preferred method to fabricate 1D nanostructures is the templated electrodeposition due to its low cost, high volume and the ability to accurately control the amount of material deposited. Methods of TiO_2 film electrodeposition from $TiOSO_4$ were developed by Natarajan and Nogami [157] and improved by Karuppuchamy *et al.* [158]; since then similar work on mainly TiO_2 films and three-dimensional nanoframes has followed [159].
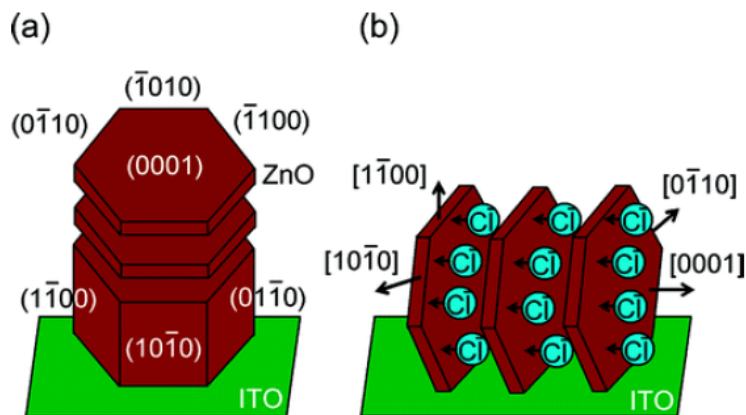
Figure 23: Schematic diagrams of (**a**) 1D and (**b**) 2D growth of ZnO nanostructures on ITO-glass. Reprinted with permission from Pradhan, D. & Leung, K. T. (2008). "Controlled Growth of Two-Dimensional and One-Dimensional ZnO Nanostructures on Indium Tin Oxide Coated Glass by Direct Electrodeposition," Langmuir 24(17), 9707–9716. Copyright (2004) American Chemical Society. All rights reserved.
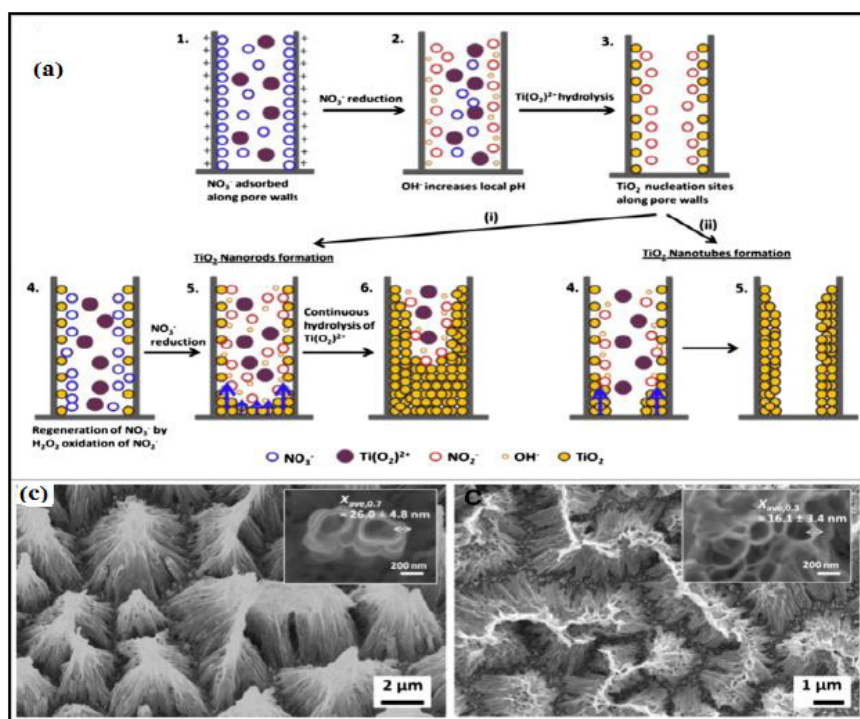
Figure 24: Schematic diagram illustrating nucleation of TiO_2 sites along pore walls of AAM (steps 1 to 3); growth of TiO_2 nanorods via route (i) steps 4 to 6 from regeneration of NO_3^- from re-oxidation of reduced NO_2^- and TiO_2 nanotubes via (ii) steps 4 to 5 confined around the pore walls from limiting reduction rates NO_3^-;(B) SEM images of as-prepared TiO_2 nanotubes. Reprinted (adapted) with permission from (from Teo, G. Y.; Ryan, M. P. & Riley, D. J. (2014). "A mechanistic study on templated electrodeposition of one-dimensional TiO2 nanorods and nanotubes using TiOSO4 as a precursor," Electrochemistry Communications 47, 13–16, ISSN: 1388-2481. Copyright (2014) Elsevier B.V. Copyright © 2013 Elsevier B.V. All rights reserved.

According with Riley *et al.* [160], the electrodeposition of TiO_2 from $TiOSO_4$ proceeds from the cathode via the reduction of NO_3^- ions (18), which leads to an increase in the local pH by generation of OH^-. This results in the hydrolysis of $Ti(O_2)SO_4$, a Ti intermediate complex formed prior to electrodeposition (19), to produce a hydroxide precipitate that subsequently via condensation and heat treatment yields TiO_2(20).

$$NO_3^-(ads) + H_2O + 2e^- \rightarrow NO_2^-(ads) + 2OH^- \qquad (18)$$

$$TiOSO_4 + H_2O_2 \rightarrow Ti(O_2)SO_4 + H_2O \text{ (red solution)} \qquad (19)$$

$$TiOSO_4 + 2OH\text{-} + (X+1)(H_2O) \rightarrow Ti(OH)_2. X (H_2O) + H_2O_2 \ SO_4^{2-} \xrightarrow{\Delta} TiO_2 \qquad (20)$$
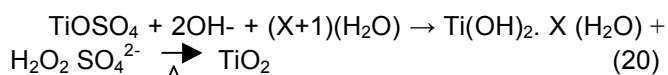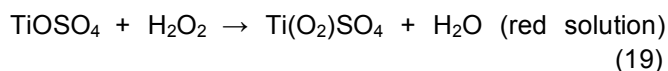
In Figure **24** the routes (i) and (ii) illustrate the proposed deposition mechanisms of TiO_2 nanorods and nanotube formation, respectively.

5. CONCLUSIONS

Templated electrosynthesis is proving to be an easy and powerful method to fabricate a variety of nanomaterials and porous structures. Using this technique, many material parameters such as dimensions and crystallinity can be tuned. The template-free electrodeposition can directly grow free-standing 1D nanostructures and their oriented arrays on the conductive substrate. It does not require the complicated pre- and post- treatments which are necessary in the template-assisted electrodeposition process. Therefore, it is simpler and more cost-effective compared with the template assisted electrodeposition. Each technique has certain characteristic advantages, and it is unlikely that a single technique will dominate all areas of application.

REFERENCES

[1] Ronaldo Fereira do Nascimento, Odair Pastor Ferreira, Amauri Jardim De Paula, Vicente de Oliveira Sousa Neto, In Advanced Nanomaterials, Nanomaterials Applications for Environmental Matrices, Elsevier, 2019, Pages 489-508, ISBN 9780128148297,https://doi.org/10.1016/B978-0-12-814829-7.00027-6. (http://www.sciencedirect.com/science/article/pii/B978012814 8297000276)

[2] Li, Y, Xu,J., Liu,H., Song,J., Li, Y. Cheng, B., Li,J.1, Li, X. 2017.A template/electrochemical deposition method for fabricating silver nanorod arrays based on porous anodic alumina. Nanomaterials and Nanotechnology.7,1-7.

https://doi.org/10.1177/1847980417717543

[3]   Chen, M.S.; Fan, F.Y.; Lin, C.K.; Chen, C.C. Enhanced Diffusion Bonding Between High Purity Aluminum and 6061 Aluminum by Electrolytic Polishing Assistance. Int. J. Electrochem. Sci. 2016, 11, 4922-4929..
https://doi.org/10.20964/2016.06.73

[4]   Ide, S.; Capraz, Ö.Ö.; Shrotriya, P.; Hebert, K.R. Oxide Microstructural Changes Accompanying Pore Formation during Anodic Oxidation of Aluminum. Electrochim. Acta 2017, 232, 303-309.
https://doi.org/10.1016/j.electacta.2017.02.113

[5]   Muench, F. Metal Nanotube/Nanowire-Based Unsupported Network Electrocatalysts. Catalysts 2018, 8, 597.
https://doi.org/10.3390/catal8120597

[6]   Galstyan, V.; Comini, E.; Ponzoni, A.; Sberveglieri, V.; Sberveglieri, G. ZnO Quasi-1D Nanostructures: Synthesis, Modeling, and Properties for Applications in Conductometric Chemical Sensors. Chemosensors 2016, 4, 6..
https://doi.org/10.3390/chemosensors4020006

[7]   Hun, C.W.; Chiu, Y.-J.; Luo, Z.; Chen, C.C.; Chen, S.H. A New Technique for Batch Production of Tubular Anodic Aluminum Oxide Films for Filtering Applications. Appl. Sci. 2018, 8, 1055.
https://doi.org/10.3390/app8071055

[8]   Tatsi,E. Griffini,G.2019.Polymeric materials for photon management in photovoltaics,Solar Energy Materials and Solar Cells,196,Pages 43-56.
https://doi.org/10.1016/j.solmat.2019.03.031

[9]   Liu, M., Peng,T., Li, H., Zhao, L., Sang, Y., Feng,Q., Xu, L., Jiang, Y., Liu, H., Zhang, J., 2019.Photoresponsive nanostructure assisted green synthesis of organics and polymers,Applied Catalysis B: Environmental, 249, 172-210,
https://doi.org/10.1016/j.apcatb.2019.02.071

[10]   Konishi, Y.; Motoyama, M.; Matsushima, H.; Fukunaka, Y.; Ishii, R. & Ito, Y., (2003). "Electrodeposition of Cu nanowire arrays with a template," J. Electroanalytical Chemistry 559, 149-153, ISSN: 0022-0728.
https://doi.org/10.1016/S0022-0728(03)00157-8

[11]   Rahman, I. Z.; Razeeb, K. M.; Kamruzzaman, M. & Serantoni M. (2004). "Characterisation of electrodeposited nickel nanowires using NCA template," J. Materials Processing Technology 153-154, 811-815, ISSN: 0924-0136.
https://doi.org/10.1016/j.jmatprotec.2004.04.168

[12]   Rabin, O.; Herz, P. R.; Lin, Y.-M.; Akinwande, A. I.; Cronin, S. B. & Dresselhaus, M. S. (2003). "Formation of Thick Porous Anodic Alumina Films and Nanowire Arrays on Silicon Wafers and Glass," Advanced Functional Materials 13, 631-638, ISSN: 1616-3028.
https://doi.org/10.1002/adfm.200304394

[13]   She, G.; Shi, W.; Zhang, X.; Wong, T.; Cai, Y. & Wang, N. (2009). "Template-Free Electrodeposition of One-Dimensional Nanostructures of Tellurium," Crystal Growth & Design 9(2), 663-666, ISSN: 1528-7505.
https://doi.org/10.1021/cg800948w

[14]   Oliveira, C. P.; Freitas, R. G.; Mattoso, L. H. C. & Pereira, E. C. (2008). "Nanostructured Materials Synthesized Using Electrochemical Techniques". In Nanostructured Materials in Electrochemistry; Eftekhari, A., Ed.; Wiley-Vch Verlag GmbH & Co. KGaA: Weinheim: Germany, Chapter 2, pp. 117-186, ISBN: 978-3-527-62150-7.
https://doi.org/10.1002/9783527621507.ch2

[15]   Vázquez, L.; Creus, A. H.; Carro, P.; Ocon, P.; Herrasti, P.; Palacio, C.; Vara, J. M.; Salvarezza, R. C. & Arvia, A. J. (1992). "Scanning Tunneling Microscopy and Scanning Electron Microscopy Observations of the Early Stage of Silver Deposition on Graphite Single Crystal Electrodes," J. Phys. Chem. 96, 10454-10460, ISSN: 1089-7690.
https://doi.org/10.1021/j100204a062

[16]   Pötzschke, R. T.; Gervasi, C. A.; Vinzelberg, S.; Staikov, G. & Lorenz, W. J. (1995). "Nanoscale Studies of Electrodeposition on HOPG (0001)," Electrochimica Acta 40(10), 1469-1474, ISSN: 0013-4686.
https://doi.org/10.1016/0013-4686(95)00049-K

[17]   Zoval, J. V.; Stiger, R. M.; Biernacki, P. R. & Penner, R. M. (1996). "Electrochemical Deposition of Silver Nanocrystallites on the Atomically Smooth Graphite Basal Plane" J. Phys. Chem. 100, 837-844, ISSN: 1089-7690.
https://doi.org/10.1021/jp952291h

[18]   Martín, H.; Carro, P.; Creus, A. H.; González, S.; Salvarezza, R. C. & Arvia, A. J. (1997). "Growth Mode Transition Involving a Potential-Dependent Isotropic to Anisotropic Surface Atom Diffusion Change. Gold Electrodeposition on HOPG followed by STM," Langmuir 13(1), 100-110, ISSN: 1520-5827.
https://doi.org/10.1021/la960700a

[19]   Zach, M. P.; Ng, K. H. & Penner, R. M. (2000). "Molybdenum Nanowires by Electrodeposition," Science 290, 2120-2123, ISSN: 1095-9203.
https://doi.org/10.1126/science.290.5499.2120

[20]   Gimeno, Y.; Creus, A. H.; González, S.; Salvarezza, R. C. & Arvia, A. J. (2001). "Preparation of 100-160-nmsized Branched Palladium Islands with Enhanced Electrocatalytic Properties on HOPG," Chem. Mat. 13(5), 1857-1864, ISSN: 1520-5002.
https://doi.org/10.1021/cm0100164

[21]   Gimeno, Y.; Creus, A. H.; Carro, P.; González, S.; Salvarezza, R. C. & Arvia, A. J. (2002). "Electrochemical Formation of Palladium Islands on HOPG: Kinetics, Morphology, and Growth Mechanisms," J. Phys. Chem. B 106(16), 4232-4244, ISSN: 1520-5207.
https://doi.org/10.1021/jp014176e

[22]   Favier, F.; Walter, E. C.; Zach, M. P.; Benter, T. & Penner, R. M. (2001). "Hydrogen Sensors and Switches from Electrodeposited Palladium Mesowire Arrays," Science 293, 2227-2231, ISSN: 1095-9203.
https://doi.org/10.1126/science.1063189

[23]   Zoval, J. V.; Lee, J.; Gorer, S. & Penner, R. M. (1998). "Electrochemical Preparation of Platinum Nanocrystallites with Size Selectivity on Basal Plane Oriented Graphite Surfaces," J. Phys. Chem. B 102(7), 1166-1175, ISSN: 1520-5207.
https://doi.org/10.1021/jp9731967

[24]   Bengough, G. D. & Stuart, J. M. (1923). Brit. Patent 223, 994.

[25]   Thompson, G. E. & Wood, G. C. (1983). "Anodic Films on Aluminium". In Treatise on Materials Science and Technology, Vol. 23, Corrosion: Aqueous Process and Passive Films; Scully, J. C., Ed.; Academic Press Inc., New York, Chapter 5, pp. 205-329, ISBN: 978-0-12-633670-2.
https://doi.org/10.1016/B978-0-12-633670-2.50010-3

[26]   Despic, A. & Parkhutik, V. P. (1989). "Electrochemistry of Aluminum in Aqueous Solutions and Physics of its Anodic Oxide". In Modern Aspects of Electrochemistry; Bokris, J. O'M., White, R. E. & Conwa, B. E., Eds.; Plenum Press: New York, Vol. 23, Chapter 6, pp. 401-503, ISBN: 978-1-4684-8762-6.
https://doi.org/10.1007/978-1-4684-8762-6_6

[27]   Martin, C. R. (1996). "Membrane-Based Synthesis of Nanomaterials" Chem. Mater. 8, 1739-1746, ISSN: 1520-5002.
https://doi.org/10.21236/ADA309882

[28]   Mawlawi, D.; Coombs, N. & Moskovits, M. (1991). "Magnetic properties of iron deposited into anodic aluminum oxide pores as a function of particle size Al," J. Applied Physics 70(8), 4421-4425, ISSN: 1089-7550.
https://doi.org/10.1063/1.349125

[29]   Tsuya, N.; Tokushima, T.; Shiraki, M.; Wakui, Y.; Saito, Y.; Nakamura, H.; Hayano, S.; Furugori, A. & Tanaka, M. (1986). "Alumite disc using anodic oxidation," IEEE Transactions on Magnetics MAG-22, 1140-1144, ISSN: 0018-9464.
https://doi.org/10.1109/TMAG.1986.1064316

[30]   Kawai, S., (1988). Proc. Electrochem. Soc. (Proc. Symp. Electrochem. Technol. Electron., 1987), 88-23, 389-400.

[31]   Spratt, G. W. D.; Bissell, P. R.; Chantrell, R. W. & Wohlfarth, E. P. (1988). "Static and Dynamic Experimental Studies of Particulate Recording Media" J. Magnetism and Magnetic Materials 75, 309-318, ISSN: 1873-4766.
https://doi.org/10.1016/0304-8853(88)90036-4

[32]   Samwel, E. O.; Bissell, P. R. & Lodder, J. C. (1993). "Remanent magnetic measurements on perpendicular recording materials with compensation for demagnetizing fields," J. Applied Physics 73(3), 1353-1359, ISSN: 1089-7550.
https://doi.org/10.1063/1.353255

[33]   Li, F.; Bao, X.; Metzger, R. M. & Carbucicchio, M. (1996). "Lanthanide and boron oxide-coated α-Fe particles," J. Applied Physics 79(8), 4869-4871, ISSN: 1089-7550.
https://doi.org/10.1063/1.361924

[34]   Li, F. & Metzger, R. M. (1997). "Activation volume of α-Fe particles in alumite films," J. Applied Physics 81, 3806-3808, ISSN: 1089-7550.
https://doi.org/10.1063/1.364776

[35]   Masuda, H. & Satoh, M. (1996). "Fabrication of Gold Nanodot Array Using Anodic Porous Alumina as an Evaporation Mask," Japanese J. Applied Physics 35, L126, ISSN: 1347-4065.
https://doi.org/10.1143/JJAP.35.L126

[36]   Masuda, H. & Fukuda, K. (1995). "Ordered Metal Nanohole Arrays Made by a Two-Step Replication of Honeycomb Structures of Anodic Alumina," Science 268, 1466-1468, ISSN: 1095-9203.
https://doi.org/10.1126/science.268.5216.1466

[37]   Diggle, J. W.; Downie, T. C. & Goulding, C. W. (1969). "Anodic oxide films on aluminum," Chemical Reviews 69(3), 365-405, ISSN: 1520-6890.
https://doi.org/10.1021/cr60259a005

[38]   Keller, F.; Hunter, M. S. & Robinson, D. L. (1953). "Structural Features of Oxide Coatings on Aluminum," J. Electrochem. Soc. 100(9), 411-419, ISSN: 1945-7111.
https://doi.org/10.1149/1.2781142

[39]   Thompson, G. E. (1997). "Porous anodic alumina: fabrication, characterization and applications," Thin Solid Films 297(1-2), 192-201, ISSN: 0040-6090.
https://doi.org/10.1016/S0040-6090(96)09440-0

[40]   Osamu, N.; Tatsuya, K.; Shungo, N. & Ryosuke, S. (2013). "Rapid fabrication of self-ordered porous alumina with 10-/sub-10-nm-scale nanostructures by selenic acid anodizing" Scientific Reports 3: 2748, 1-6, ISSN: 2045-2322.
https://doi.org/10.1038/srep02748

[41]   Kape, J. M. (1961). "Unusual anodizing processes and their practical significance," Electroplating & Metal Finishing 14, 407-415, ISSN: 0013-5305.

[42]   Keller, F.; Hunter, M. S. & Robinson, D. L. (1953). "Structural features of oxide coatings on aluminum," J. Electrochem. Soc. 100, 411-419, ISSN: 1945-7111.
https://doi.org/10.1149/1.2781142

[43]   Chu, S. Z.; Wada, K.; Inoue, S.; Isogai, M.; Katsuta, Y. & Yasumori, A. (2006). "Large-Scale Fabrication of Ordered Nanoporous Alumina Films with Arbitrary Pore Intervals by Critical-Potential Anodization," J. Electrochem. Soc. 153(9), B384-B391, ISSN: 1945-7111.
https://doi.org/10.1149/1.2218822

[44]   Lee, W.; Nielsch, K. & Gösele, U. (2007). "Self-ordering behavior of nanoporous anodic aluminum oxide (AAO) in malonic acid anodization," Nanotechnology 18(47), 475713, ISSN: 1361-6528.
https://doi.org/10.1088/0957-4484/18/47/475713

[45]   Verwey, E. J. W. (1935). "Electrolytic conduction of a solid insulator at high voltages-formation of the anodic oxide film on aluminum," Physica (The Hague) 2, 1059-1063.
https://doi.org/10.1016/S0031-8914(35)90193-8

[46]   Mott, N. F. (1947). "Theory of the formation of protective oxide films on metals - III," Trans. Faraday Soc. 43, 429-434.
https://doi.org/10.1039/TF9474300429

[47]   Lee, W. & Park, S. -J. (2014). "Porous Anodic Aluminum Oxide: Anodization and Templated Synthesis of Functional Nanostructures," Chemical Reviews 114(15), 7487-7556, ISSN: 1520-6890.
https://doi.org/10.1021/cr500002z

[48]   Hnida, K.; Mech, J. & Sulka, G. D. (2013). "Template-assisted electrodeposition of indium-antimony nanowires - Comparison of electrochemical methods," Appl. Surface Sci. 287, 252-256, ISSN: 0169-4332.
https://doi.org/10.1016/j.apsusc.2013.09.135

[49]   Yang, Y. W.; Li, L.; Huang, X. H.; Ye, M.; Wu, Y. C. & Li, G. H. (2006). "Transport properties of InSb nanowire arrays," Appl. Phys. A 84, 7-9, ISSN: 1432-0630.
https://doi.org/10.1007/s00339-006-3585-1

[50]   Yang, Y. W., Li, L., Huang, X. H., Li, G. H., Zhang, L., (2007). "Fabrication and optical property of single-crystalline InSb nanowire arrays," J. Materials Science 42, 2753-2757, ISSN: 1573-4803.
https://doi.org/10.1007/s10853-006-1272-4

[51]   Chen, Y.-H.; Shen, Y.-M.; Wang, S.-C. & Huang, J.-L. (2014). "Fabrication of one-dimensional ZnO nanotube and nanowire arrays with an anodic alumina oxide template via electrochemical deposition," Thin Solid Films 570, Part B, 303-309, ISSN: 0040-6090.
https://doi.org/10.1016/j.tsf.2014.03.014

[52]   Schlenoff, J. B. (2006). US20067105052B1.

[53]   She, G.; Mu L. & Shi, W. (2009). "Electrodeposition of One-Dimensional Nanostructures," Recent Patents on Nanotech. 3, 182-191, ISSN: 2212-4020.
https://doi.org/10.2174/187221009789177777

[54]   Jung, T.; Schlittler, R.; Gimzewski, J. K. & Himpsel, F. J. (1995). "One-dimensional metal structures at decorated steps," Appl. Phys. A 61, 467-474, ISSN: 1432-0630.
https://doi.org/10.1007/BF01540248

[55]   Himpsel, F. J.; Jung, T.; Kirakosian, A.; Lin, J. L.; Petrovykh, D. Y.; Rauscher, H. & Viernow, J. (1999). "Nanowires by step decoration," MRS Bull 24(8), 20-24, ISSN: 1938-1425.
https://doi.org/10.1557/S0883769400052854

[56]   Blanc, M.; Kuhnke, K.; Marsico, V. & Kern, K. (1998). "Probing step decoration by grazing-incidence helium scattering," Surf. Sci. Lett. 414, L964-L969, ISSN: 0167-2584.
https://doi.org/10.1016/S0039-6028(98)00561-5

[57]   Gambardella, P.; Blanc, M.; Brune, H.; Kuhnke, K. & Kern, K. (2000). "One-dimensional metal chains on Pt vicinal surfaces," Phys. Rev. B 61, 2254-2262, ISSN: 1550-235X.
https://doi.org/10.1103/PhysRevB.61.2254

[58]   Himpsel, F. J. & Ortega, J. E. (1994). "Edge state and terrace state for Cu on W(331) and W(110)," Phys. Rev. B 50(7), 4992-4995, ISSN: 1550-235X.
https://doi.org/10.1103/PhysRevB.50.4992

[59]   Mundschau, M.; Bauer, E.; Telieps, W. & Swiech, W. (1989). "Initial epitaxial growth of copper silicide on silicon {111} studied by low-energy electron microscopy and photoemission electron microscopy," J. Applied Physics 65(12), 4747-4752, ISSN: 1089-7550.
https://doi.org/10.1063/1.343227

[60]   Penner, R. M. (2002). "Mesoscopic Metal Particles and Wires by Electrodeposition," J. Phys. Chem. B 106(13), 3339-3353, ISSN: 1520-5207.
https://doi.org/10.1021/jp013219o

[61]   Nichols, R. J.; Kolb, D. M. & Behm, R. J. (1991). "STM observations of the initial stages of copper deposition on gold single-crystal electrodes," J. Electroanalytical Chemistry Interfacial Electrochemistry 313, 109-119, ISSN: 1572-6657.
https://doi.org/10.1016/0022-0728(91)85174-N

[62]   Dekoster, J.; Degroote, B.; Pattyn, H.; Langouche, G.; Vantomme, A. & Degroote, S. (1999). "Step decoration during deposition of Co on Ag(001) by ultralow energy ion beams," Appl. Phys. Lett. 75, 938-940, ISSN: 1077-3118. https://doi.org/10.1063/1.124560

[63]   Jung, T.; Schlittler, R.; Gimzewski, J. K. & Himpsel, F. J. (1995). "One-dimensional metal structures at decorated steps," Appl. Phys. A 61(5), 467-474, ISSN: 1432-0630. https://doi.org/10.1007/BF01540248

[64]   Zach, M. P.; Ng, K. H. & Penner, R. M. (2000). "Molybdenum nanowires by electrodeposition," Science 290, 2120-2123, ISSN: 1095-9203. https://doi.org/10.1126/science.290.5499.2120

[65]   Menke, E. J.; Li, Q. & Penner, R. M. (2004). "Bismuth telluride (Bi2Te3) nanowires synthesized by cyclic electrodeposition/stripping coupled with step edge decoration," Nano Lett. 4, 2009-2014, ISSN: 1530-6992. https://doi.org/10.1021/nl048627t

[66]   Pandey, R. K.; Sahu, S. N. & Chandra, S. (1996). "Handbook of semiconductor electrodeposition". CRC Press, Marcel Dekker Inc., 304 p. ISBN: 978-0-824-79701-0.

[67]   Morin, S.; Lachenwitzer, A.; Magnussen, O. M. & Behm, R. J. (1999). "Potential-Controlled Step Flow to 3D Step Decoration Transition: Ni Electrodeposition on Ag(111)," Phys. Rev. Lett. 83, 5066-5069, ISSN: 1079-7114. https://doi.org/10.1103/PhysRevLett.83.5066

[68]   Otero, R.; Rosei, F.; Naitoh, Y.; Jiang, P.; Thostrup, P.; Gourdon, A.; Laegsgaard, E.; Stensgaard, I.; Joachim, C. & Besenbacher, F. (2004). "Nanostructuring Cu Surfaces Using Custom-Designed Molecular Molds," Nano Lett. 4(1), 75-78, ISSN: 1530-6992. https://doi.org/10.1021/nl0348793

[69]   Gates, B. D.; Xu, Q.; Stewart, M.; Ryan, D.; Willson, C. G. & Whitesides, G. M. (2005). "New Approaches to Nanofabrication: Molding, Printing, and Other Techniques," Chemical Reviews 105(4), 1171-1196, ISSN: 1520-6890. https://doi.org/10.1021/cr030076o

[70]   Li, Q.; Newberg, J. T.; Walter, E. C.; Hemminger, J. C. & Penner, R. M. (2004). "Polycrystalline Molybdenum Disulfide (2H−MoS2) Nano- and Microribbons by Electrochemical/Chemical Synthesis," Nano Lett. 4(2), 277-281, ISSN: 1530-6992. https://doi.org/10.1021/nl035011f

[71]   Li, Q.; Olson, J. B. & Penner, R. M. (2004). "Nanocrystalline α-MnO2 Nanowires by Electrochemical Step-Edge Decoration," Chem. Mater. 16(18), 3402-3405, ISSN: 1520-5002. https://doi.org/10.1021/cm049285v

[72]   Favier, F.; Walter, E. C.; Zach, M. P.; Benter, T. & Penner, R. M. (2001). "Hydrogen Sensors and Switches from Electrodeposited Palladium Mesowire Arrays," Science 293, 2227-2231, ISSN: 1095-9203. https://doi.org/10.1126/science.1063189

[73]   Price, P. B. & Walker, R. M. (1962). "Chemical etching of charged-particle tracks in solids," J. Applied Physics 33, 3407-3412, ISSN: 1089-7550. https://doi.org/10.1063/1.1702421

[74]   Fleischer, R. L. & Price, P. B. (1963). "Charged particle tracks in glass," J. Applied Physics 34, 2903-2904, ISSN: 1089-7550. https://doi.org/10.1063/1.1729828

[75]   Fleischer, R. L.; Price, P. B. & Walker, R. M. (1975). "Nuclear tracks in solids: principles and applications". University of California Press, 605 p. ISBN: 0-520-02665-9. https://doi.org/10.1525/9780520320239

[76]   Chien, C. L.; Searson, P. S. C. & Liu, K. (2001). US20016187165.

[77]   Sager, B. M. & Roscheisen, M. R. (2005). US20056852920B2.

[78]   Martin, C. R. (1996). "Membrane-Based Synthesis of Nanomaterials," Chem. Mater. 8(8), 1739-1746, ISSN: 1520-5002. https://doi.org/10.21236/ADA309882

[79]   Brumlik, C. J. & Martin, C. R. (1991). "Template Synthesis of Metal Microtubules," J. Am. Chem. Soc. 113(8), 3174-3175, ISSN: 1520-5126. https://doi.org/10.21236/ADA232827

[80]   Chakarvarti, S. K. & Vetter, J. (1993). "Microfabrication of metal-semiconductor heterostructures and tubules using nuclear track filters," J. Micromechanics Microengineering 3, 57-59, ISSN: 1361-6439. https://doi.org/10.1088/0960-1317/3/2/004

[81]   Chakarvarti, S. K. & Vetter, J. (1991). "Morphology of etched pores and microstructures fabricated from nuclear track filters," J. Nuclear Instruments Methods in Physics Research B 62, 109-115, ISSN: 0168-583X. https://doi.org/10.1016/0168-583X(91)95936-8

[82]   Tian, M.; Wang, J.; Kumar, N.; Han, T.; Kobayashi, Y.; Liu, Y.; Mallouk, T. E. & Chan, M. H. W. (2006). "Observation of Superconductivity in Granular Bi Nanowires Fabricated by Electrodeposition," Nano Lett. 6(12), 2773-2780, ISSN: 1530-6992. https://doi.org/10.1021/nl0618041

[83]   Molares, M. E. T.; Buschmann, V.; Dobrev, D.; Neumann, R.; Scholz, R.; Schuchert, I. U. & Vetter, J. (2001). "Single-crystalline copper nanowires produced by electrochemical deposition in polymeric ion track membranes," Advanced Materials 13(1), 62-65, ISSN: 1521-4095. https://doi.org/10.1002/1521-4095(200101)13:1<62::AID-ADMA62>3.0.CO;2-7

[84]   Sander, M. S. & Gao, H. (2005). "Aligned Arrays of Nanotubes and Segmented Nanotubes on Substrates Fabricated by Electrodeposition onto Nanorods," J. Am. Chem. Soc. 127(35), 12158-12159, ISSN: 1520-5126. https://doi.org/10.1021/ja0522231

[85]   Hernández, R. M.; Richter, L.; Semancik, S.; Stranick, S. & Mallouk, T. E. (2004). "Template Fabrication of Protein-Functionalized Gold-Polypyrrole-Gold Segmented Nanowires," Chem. Mater. 16(18), 3431-3438, ISSN: 1520-5002. https://doi.org/10.1021/cm0496265

[86]   Xia, Y. N.; Yang, P. D.; Sun, Y. G.; Wu, Y. Y.; Mayers, B.; Gates, B.; Yin, Y. D.; Kim, F. & Yan, H. Q. (2003). "One-Dimensional Nanostructures: Synthesis, Characterization, and Applications," Advanced Materials 15(5), 353-389, ISSN: 1521-4095. https://doi.org/10.1002/adma.200390087

[87]   Feng, Z.; Zhang, Q.; Lin, L.; Guo, H.; Zhou, J. & Lin, Z. (2010). "（0001）-Preferential Growth of CdSe Nanowires on Conducting Glass: Template-Free Electrodeposition and Application in Photovoltaics," Chem. Mater. 22(9), 2705-2710, ISSN: 1520-5002. https://doi.org/10.1021/cm901703d

[88]   Tena-Zaera, R.; Katty, A.; Bastide, S. & Levy-Clement, C. (2007). "Annealing Effects on the Physical Properties of Electrodeposited ZnO/CdSe Core-Shell Nanowire Arrays," Chem. Mat. 19(7), 1626-1632, ISSN: 1520-5002. https://doi.org/10.1021/cm062390f

[89]   He, Z.; Jie, J.; Zhang, W.; Zhang, W.; Luo, L.; Fan, X.; Yuan, G.; Bello, I. & Lee, S.-T. (2009). "Tuning electrical and photoelectrical properties of CdSe nanowires via indium doping," Small 5(3), 345-350, ISSN: 1613-6810. https://doi.org/10.1002/smll.200801006

[90]   Ma, C. & Wang, Z. L. (2005). "Road map for the controlled synthesis of CdSe nanowires, nanobelts, and nanosaws - a step towards," Advanced Materials 17(21), 2635-2639, ISSN: 1521-4095. https://doi.org/10.1002/adma.200500805

[91]   Wang, G. X.; Park, M. S.; Liu, H. K.; Wexler, D. & Chen, J. (2006). "Synthesis and characterization of one-dimensional

CdSe nanostructures," Appl. Phys. Lett. 88(19), 193115, ISSN: 1077-3118.
https://doi.org/10.1063/1.2202725

[92]   She, G.; Zhang, X.; Shi, W.; Cai, Y.; Wang, N.; Liu, P. & Chen, D. (2008). "Template-Free Electrochemical Synthesis of Single-Crystal CuTe Nanoribbons," Crystal Growth & Design 8(6), 1789-1791, ISSN: 1528-7505.
https://doi.org/10.1021/cg7008623

[93]   (a) Shi, W. S. & She, G. W. (2008): CN10100983.0.(b) Algarni, Z.; Singh, A.; Philipose, U. Synthesis of Amorphous InSb Nanowires and a Study of the Effects of Laser Radiation and Thermal Annealing on Nanowire Crystallinity. Nanomaterials 2018, 8, 607.
https://doi.org/10.3390/nano8080607

[94]   Shi, W. S. & She, G. W. (2008): CN101009826.

[95]   Tadros, Th. F. (Ed.) (1984). In Surfactants, Academic Press, London, 342 p. ISBN: 978-0-12682.

[96]   Attard, G. S.; Bartlett, P. N.; Coleman, N. R. B.; Elliott, J. M.; Owen, J. R. & Wang, J. H. (1997). "Mesoporous platinum films from lyotropic liquid crystalline phases," Science 278, 838-840, ISSN: 1095-9203.
https://doi.org/10.1126/science.278.5339.838

[97]   Bartlett, P. N. & Marwan, J. (2003). "Electrochemical Deposition of Nanostructured (H1-e) Layers of Two Metals in Which Pores within the Two Layers Interconnect," Chem. Mater. 15(15), 2962-2968, ISSN: 1520-5002.
https://doi.org/10.1021/cm0210400

[98]   Bartlett, P. N. & Marwan, J. (2003). "Preparation and characterization of H1-e rhodium films," Microporous Mesoporous Materials. 62(1-2), 73-79, ISSN 1387-1811.
https://doi.org/10.1016/S1387-1811(03)00394-9

[99]   Braun, P. V.; Osenar, P.; Twardowski, M.; Tew, G. N. & Stupp, S. I. (2005). "Macroscopic Nanotemplating of Semiconductor Films with Hydrogen-Bonded Lyotropic Liquid Crystals," Advanced Functional Materials 15(11), 1745-1750, ISSN: 1616-3028.
https://doi.org/10.1002/adfm.200500083

[100] Shin, H. -C.; Dong, J. & Liu, M. (2003). "Nanoporous Structures Prepared by an Electrochemical Deposition Process," Advanced Materials 15(19), 1610-1614, ISSN: 1521-4095.
https://doi.org/10.1002/adma.200305160

[101] Xu, L.; Tung, L. D.; Spinu, L.; Zakhidov, A. A.; Baughman, R. H. & Wiley, J. B. (2003). "Synthesis and Magnetic Behavior of Periodic Nickel Sphere Arrays," Advanced Materials 15(18), 1562-1564, ISSN: 1521-4095.
https://doi.org/10.1002/adma.200305030

[102] Lai, M.; Kulak, A. N.; Law, D.; Zhang, Z.; Meldrum, F. C. & Riley, D. J. (2007). "Profiting from nature: macroporous copper with superior mechanical properties," Chem. Commun., 3547-3549, ISSN: 1364-548X.
https://doi.org/10.1039/b707469g

[103] Zhu, J.; Gui, Z. & Ding, Y., (2008). "A simple route to lanthanum hydroxide nanorods," Mat. Lett. 62(16), 2373-2376, ISSN: 0167-577X.
https://doi.org/10.1016/j.matlet.2007.12.002

[104] Deng, J.; Zhang, L.; Au, C. T. & Dai, H. (2009). "Template-free synthesis of high surface area single-crystalline lanthanum hydroxide nanorods via a low-temperature solution route," Mat. Lett. 63(6-7), 632-634, ISSN: 0167-577X.
https://doi.org/10.1016/j.matlet.2008.12.005

[105] Ma, X.; Zhang, H.; Ji, Y.; Xu, J. & Yang, D. (2004). "Synthesis of ultrafine lanthanum hydroxide nanorods by a simple hydrothermal process," Mat. Lett. 58, 1180-1182, ISSN: 0167-577X.
https://doi.org/10.1016/j.matlet.2003.08.031

[106] Yao, C.-Z.; Wei, B.-H.; Ma, H.-X.; Gong, Q.-J.; Jing, K.-W.; Sun, H. & Meng, L.-X. (2011). "Facile fabrication of La (OH) 3 nanorod arrays and their application in wastewater

treatment," Mat. Lett. 65(3), 490-492, ISSN: 0167-577X.
https://doi.org/10.1016/j.matlet.2010.10.065

[107] González-Rovira, L.; Sánchez-Amaya, J. M.; López-Haro, M.; Hungria, A. B.; Boukha, Z.; Bernal, S. & Botana, F. J. (2008). "Formation and characterization of nanotubes of La(OH)3 obtained using porous alumina membranes," Nanotechnology 19, 495305-495314, ISSN: 1361-6528.
https://doi.org/10.1088/0957-4484/19/49/495305

[108] Zheng, D.; Shi, J.; Lu, X.; Wang, C.; Liu, Z.; Liang, C.; Liu, P. & Tong, Y. (2010). "Controllable growth of La(OH)3 nanorod and nanotube arrays," Crystal Engineering Communications 12, 4066-4070, ISSN: 1466-8033.
https://doi.org/10.1039/c0ce00247j

[109] Bocchetta, P.; Santamaria, M. & Quarto, F. D. (2007). "Template electrosynthesis of La(OH)3 and Nd(OH)3 nanowires using porous anodic alumina membranes," Electrochemistry Communications 9, 683-688, ISSN: 1388-2481.
https://doi.org/10.1016/j.elecom.2006.10.053

[110] Tissue, B. M. (1998). "Synthesis and Luminescence of Lanthanide Ions in Nanoscale Insulating Hosts," Chem. Mat. 10(10), 2837-2845, ISSN: 1520-5002.
https://doi.org/10.1021/cm9802245

[111] Mao, G.; Zhang, H.; Li, H.; Jin, J. & Niu, S. (2012). "Selective Synthesis of Morphology and Species Controlled La2O3:Eu3+ and La2O2CO3:Eu3+ Phosphors by Hydrothermal Method," J. Electrochem. Soc. 159(3), J48-J53, ISSN: 1945-7111.
https://doi.org/10.1149/2.031203jes

[112] Murray, E. P.; Tsai, T. & Barnett, S. A. (1999). "A direct-methane fuel cell with a ceria-based anode," Nature 400, 649-651, ISSN: 1476-4687.
https://doi.org/10.1038/23220

[113] Orr, G. W.; Barbour, L. J. & Atwood, J. L. (1999). "Controlling Molecular Self-Organization: Formation of Nanometer-Scale Spheres and Tubules," Science 285, 1049-1052, ISSN: 1095-9203.
https://doi.org/10.1126/science.285.5430.1049

[114] Liu, Z.; Zheng, D.; Su, Y.; Liu, Z. & Tong, Y. (2010). "Facile and Efficient Electrochemical Synthesis of Lanthanum Hydroxide Nanospindles and Nanorods," Electrochem. Solid-State Letters 13(12), E15-E18, ISSN: 1099-0062.
https://doi.org/10.1149/1.3486446

[115] Aghazadeh, M.; Arhami, B.; Barmi, A.-A. M.; Hosseinifard, M.; Gharailou, D. & Fathollahi, F. (2014). "La(OH)3 and La2O3 nanospindles prepared by template-free direct electrodeposition followed by heat-treatment," Mat. Lett. 115, 68-71, ISSN: 0167-577X.
https://doi.org/10.1016/j.matlet.2013.10.002

[116] Robinson, T.; McMullan, G.; Marchant, R. & Nigam, P. (2001). "Remediation of dyes in textile effluent: a critical review on current treatment technologies with a proposed alternative.," Biores. Technology 77(3), 247-255, ISSN 0960-8524.
https://doi.org/10.1016/S0960-8524(00)00080-8

[117] Pearce, C. I.; Lloyd, J. R. & Guthrie, J. T. (2003). "The removal of colour from textile wastewater using whole bacterial cells: a review," Dyes and Pigments 58(3), 179-196, ISSN: 0143-7208.
https://doi.org/10.1016/S0143-7208(03)00064-0

[118] Ayed, L.; Chaieb, K.; Cheref, A. & Bakhrouf, A. (2009). "Biodegradation of triphenylmethane dye Malachite Green by Sphingomonas paucimobilis," World J. Microbiology and Biotechnology 25, 705-711, ISSN: 1573-0972.
https://doi.org/10.1007/s11274-008-9941-x

[119] Konstantinou, I. K. & Albanis, T. A. (2004). "TiO2-assisted photocatalytic degradation of azo dyes in aqueous solution: kinetic and mechanistic investigations: A review," Applied Catalysis B: Environmental 49(1), 1-14, ISSN: 0926-3373.
https://doi.org/10.1016/j.apcatb.2003.11.010

[120] H., Zollinger (Ed.) (2003). Color Chemistry: Synthesis, Properties and Applications of Organic Dyes and Pigments (3rd revised ed.), Wiley-VCH, Weinheim, 637 p. ISBN: 3-906390-23-3.

[121] Akpan, U. G. & Hameed, B. H. (2009). "Parameters affecting the photocatalytic degradation of dyes using TiO2-based photocatalysts: A review," J. Haz. Mat. 170(2-3), pp. 520-529, ISSN 0304-3894.
https://doi.org/10.1016/j.jhazmat.2009.05.039

[122] Forgacs, E.; Cserháti, T. & Oros, G. (2004). "Removal of synthetic dyes from wastewaters: a review," Environment International 30, 953-971, ISSN: 0160-4120.
https://doi.org/10.1016/j.envint.2004.02.001

[123] He, Z.; Sun, C.; Yang, S.; Ding, Y.; He, H. & Wang, Z. (2009). " Photocatalytic degradation of rhodamine B by Bi2WO6 with electron accepting agent under microwave irradiation: Mechanism and pathway," J. Haz. Mat. 162(2-3), pp. 1477-1486, ISSN: 0304-3894.
https://doi.org/10.1016/j.jhazmat.2008.06.047

[124] Li, L.; Dai, W. K.; Yu, P.; Zhao, J. & Qu, Y. B. J. (2009). "Decolorisation of synthetic dyes by crude laccase from Rigidoporus lignosus W1," J. Chemical Technology Biotechnlogy 84(3), 399-404, ISSN: 1097-4660.
https://doi.org/10.1002/jctb.2053

[125] Arslan, I. & Balcioglu, A. I. (2001). "Advanced oxidation of raw and biotreated textile industry wastewater with O3, H2O2/UV-C and their sequential application," J. Chemical Technology Biotechnlogy 76(1), 53-60, ISSN: 1097-4660.
https://doi.org/10.1002/1097-4660(200101)76:1<53::AID-JCTB346>3.0.CO;2-T

[126] Dhir, A.; Prakash, N. T. & Sud, D. (2012). "Comparative studies on TiO2/ZnO photocatalyzed degradation of 4-chlorocatechol and bleach mill effluents," Desalination and Water Treatment 46(1-3), 196-204, ISSN: 1944-3986.
https://doi.org/10.1080/19443994.2012.677521

[127] Ladanov, M.; Ram, M. K.; Matthews, G. & Kumar, A. (2011). "Structure and Opto-electrochemical Properties of ZnO Nanowires Grown on n-Si Substrate," Langmuir 27(14), 9012-9017, ISSN: 1520-5827.
https://doi.org/10.1021/la200584j

[128] Lin, D.; Wu, H.; Zhang, R. & Pan, W. (2009). "Enhanced Photocatalysis of Electrospun Ag−ZnO Heterostructured Nanofibers," Chem. Mat. 21(15), 3479-3484, ISSN: 1520-5002.
https://doi.org/10.1021/cm900225p

[129] Evgenidou, E.; Fytianos, K. & Poulios, I. (2005). "Semiconductor-sensitized photodegradation of dichlorvos in water using TiO2 and ZnO as catalysts," Applied Catalysis B: Environmental 59(1-2), 81-89, ISSN: 0926-3373.
https://doi.org/10.1016/j.apcatb.2005.01.005

[130] Baruah, S.; Mahmood, M. A.; Myint, M. T. Z.; Bora, T. & Dutta, J. (2010). "Enhanced visible light photocatalysis through fast crystallization of zinc oxide nanorods," Beilstein J. Nanotechnology. 1, 14-20, ISSN: 2190-4286.
https://doi.org/10.3762/bjnano.1.3

[131] Baruah, S.; Rafique, F. F. & Dutta, J. (2008). "Visible light photocatalysis by tailoring crystal defects in zinc oxide nanostructures," Nano 3(05), 399-407, ISSN: 1793-7094.
https://doi.org/10.1142/S179329200800126X

[132] Zhang, Y.; Ram, M. K.; Stefanakos, E. K. & Goswami, D. Y. (2012). "Synthesis, Characterization, and Applications of ZnO Nanowires," J. Nanomaterials. 2012, 624520, ISSN: 1687-4129.
https://doi.org/10.1155/2012/624520

[133] Hornyak, G. L.; Dutta, J.; Tibbals, H. & Rao, A. K., (Eds.) (2008). Introduction to Nanoscience, CRC Press, Boca Raton, 815 p. ISBN 978-1-4200-4805-6.

[134] O'Regan, B. & Graetzel, M. (1991). "A low-cost, high-efficiency solar cell based on dye-sensitized colloidal titanium dioxide films," Nature 353 (6346), 737-740, ISSN: 1476-4687.
https://doi.org/10.1038/353737a0

[135] Gratzel, M. (2001). "Photoelectrochemical cells," Nature 414 (6861), 338-344, ISSN: 1476-4687.
https://doi.org/10.1038/35104607

[136] Peter, L. M. (2007). "Characterization and Modeling of Dye-Sensitized Solar Cells," J. Physical Chemistry C 111(18), 6601-6612, ISSN: 1932-7455.
https://doi.org/10.1021/jp069058b

[137] Baxter, J. B. & Aydil, E. S. (2005). "Nanowire-based dye-sensitized solar cells," Appl. Phys. Lett. 86(5), 053114, ISSN: 1077-3118.
https://doi.org/10.1063/1.1861510

[138] Zhang, Q.; Dandeneau, C. S.; Zhou, X. & Cao, G. (2009). "ZnO Nanostructures for Dye-Sensitized Solar Cells," Advanced Materials 21(41), 4087-4108, ISSN: 1521-4095.
https://doi.org/10.1002/adma.200803827

[139] Nissfolk, J.; Fredin, K.; Hagfeldt, A. & Boschloo, G. (2006). "Recombination and Transport Processes in Dye-Sensitized Solar Cells Investigated under Working Conditions," J. Phys. Chem. B 110(36), 17715-17718, ISSN: 1520-5207.
https://doi.org/10.1021/jp064046b

[140] Law, M.; Greene, L. E.; Johnson, J. C.; Saykally, R. & Yang, P. (2005). "Nanowire dye-sensitized solar cells," Nature Materials 4(6), 455-459, ISSN: 1476-4660.
https://doi.org/10.1038/nmat1387

[141] Martinson, A. B. F.; Elam, J. W.; Hupp, J. T. & Pellin, M. J. (2007). "ZnO Nanotube Based Dye-Sensitized Solar Cells," Nano Lett., 7(8), 2183-2187, ISSN: 1530-6992.
https://doi.org/10.1021/nl070160

[142] Ozgur, U.; Alivov, Y. I.; Liu, C.; Teke, A.; Reshchikov, M. A.; Dogan, S.; Avrutin, V.; Cho, S.-J & Morkoc, H. (2005). "A comprehensive review of ZnO materials and devices," J. Applied Physics 98(4), 041301, ISSN: 1089-7550.
https://doi.org/10.1063/1.1992666

[143] Yoon, H. S.; Kim, M. H. & Seongil, J. H. (2003). "Photodetecting properties of ZnO-based thin-film transistors Bae," Appl. Phys. Lett. 83(25), 5313-5315, ISSN: 1077-3118.
https://doi.org/10.1063/1.1633676

[144] Lee, C.-H.; Chiu, W.-H.; Lee, K.-M.; Yen, W.-H.; Lin, H.-F.; Hsieh, W.-F. & Wu, J.-M. (2010). "The influence of tetrapod-like ZnO morphology and electrolytes on energy conversion efficiency of dye-sensitized solar cells," Electrochimica Acta, 55(28), 8422-8429, ISSN: 0013-4686.
https://doi.org/10.1016/j.electacta.2010.07.061

[145] Jiang, C. Y.; Sun, X. W.; Lo, G. Q.; Kwong, D. L. & Wang, J. X. (2007). "Improved dye-sensitized solar cells with a ZnO-nanoflower photoanode," Appl. Phys. Lett. 90(26), 263501, ISSN: 1077-3118.
https://doi.org/10.1063/1.2751588

[146] Baxter, J. B. & Aydil, E. S. (2006). "Dye-sensitized solar cells based on semiconductor morphologies with ZnO nanowires," Solar Energy Materials Solar Cells 90(5), 607-622, ISSN: 0927-0248.
https://doi.org/10.1016/j.solmat.2005.05.010

[147] Xu, F.; Dai, M.; Lu, Y. & Sun, L. (2010). "Hierarchical ZnO Nanowire-Nanosheet Architectures for High Power Conversion Efficiency in Dye-Sensitized Solar Cells," J. Physical Chemistry C 114(6), 2776-2782, ISSN: 1932-7455.
https://doi.org/10.1021/jp910363w

[148] Peulon, S. & Lincot, D. (1998). "Mechanistic study of cathodic electrodeposition of zinc oxide and zinc hydroxychloride films from oxygenated aqueous zinc chloride solutions," J. Electrochem. Soc. 145(3), 864-874, ISSN: 1945-7111.
https://doi.org/10.1149/1.1838359

[149] Izaki, M. & Omi, T. (1996). "Transparent zinc oxide films prepared by electrochemical reaction," Appl. Phys. Lett. 68(17), 2439-2440, ISSN: 1077-3118.
https://doi.org/10.1063/1.116160

[150] Pauporte, Th. & Lincot, D. (2001). "Hydrogen peroxide oxygen precursor for zinc oxide electrodeposition I. Deposition in perchlorate medium," J. Electrochem. Soc. 148(4), C310-C314, ISSN: 1945-7111. https://doi.org/10.1149/1.1357175

[151] Pradhan, D. & Leung, K. T. (2008). "Controlled Growth of Two-Dimensional and One-Dimensional ZnO Nanostructures on Indium Tin Oxide Coated Glass by Direct Electrodeposition," Langmuir 24(17), 9707-9716, ISSN: 1520-5827. https://doi.org/10.1021/la8008943

[152] Fujishima, A. & Honda, K. (1972). "Electrochemical photolysis of water at a semiconductor electrode ," Nature 238, 37-38, ISSN: 1476-4687. https://doi.org/10.1038/238037a0

[153] Hashimoto, K.; Irie, H. & Jujishima, A. (2005). "TiO2 Photocatalysis: A Historical Overview and Future Prospects," Japanese J. Applied Physics 44(12), 8269-8285, ISSN: 1347-4065. https://doi.org/10.1143/JJAP.44.8269

[154] Mor, G. K.; Shanker, K.; Paulose, M.; Varghese, O. K. & Grimes, C. A. (2005). "Use of Highly-Ordered TiO2 Nanotube Arrays in Dye-Sensitized Solar Cells," Nano Lett. 6(2), 215-218, ISSN: 1530-6992. https://doi.org/10.1021/nl052099j

[155] Roy, P. S. & Berger, P. S. (2011). "TiO2 nanotubes: Synthesis and applications," Angewandte Chemie International Edition 50(13), 2904-2939, ISSN: 1521-3773. https://doi.org/10.1002/anie.201001374

[156] Zhang, X.; Yao, B.; Zhao, L.; Liang, C.; Zhang, L. & Mao, Y. (2001). "Electrochemical Fabrication of Single-Crystalline Anatase TiO2 Nanowire Arrays," J. Electrochem. Soc. 148(7), G398-G400, ISSN: 1945-7111. https://doi.org/10.1149/1.1378293

[157] Natarajan, C. & Nogami, G. (1996). "Cathodic Electrodeposition of Nanocrystalline Titanium Dioxide Thin Films," J. Electrochem. Soc. 143(5), 1547-1550, ISSN: 1945-7111. https://doi.org/10.1149/1.1836677

[158] Karuppuchamy, S.; Nonomura, K.; Yoshida, T.; Sugiura, T. & Minoura, H., (2002). "Cathodic electrodeposition of oxide semiconductor thin films and their application to dye-sensitized solar cells," Solid State Ionics 151, 19-27, ISSN: 1872-7689. https://doi.org/10.1016/S0167-2738(02)00599-4

[159] Chen, Y.; Kim, H. C.; McVittie, J.; Ting, C. & Nishi, Y. (2010). "Synthesis of TiO(2) nanoframe and the prototype of a nanoframe solar cell," Nanotechnology 21(18), 185303, ISSN: 1361-6528. https://doi.org/10.1088/0957-4484/21/18/185303

[160] Teo, G. Y.; Ryan, M. P. & Riley, D. J. (2014). "A mechanistic study on templated electrodeposition of one-dimensional TiO2 nanorods and nanotubes using TiOSO4 as a precursor," Electrochemistry Communications 47, 13-16, ISSN: 1388-2481. https://doi.org/10.1016/j.elecom.2014.07.011